

## Water Resources Research

### RESEARCH ARTICLE

10.1029/2017WR021903

#### Key Points:

- Lithology and associated critical zone structure can exert primary control on wetted channel extent within a given climate
- Groundwater drainage via fractures to spring-fed wetted channel networks may be common in mountainous watersheds
- Nearby watersheds can have dramatically different summer wetted channel networks that result in fundamentally different aquatic ecosystems

#### Supporting Information:

- Supporting Information S1

#### Correspondence to:

S. M. Lovill,  
skylovill@berkeley.edu

#### Citation:

Lovill, S. M., Hahm, W. J., & Dietrich, W. E. (2018). Drainage from the critical zone: Lithologic controls on the persistence and spatial extent of wetted channels during the summer dry season. *Water Resources Research*, 54, 5702–5726. <https://doi.org/10.1029/2017WR021903>

Received 25 SEP 2017

Accepted 25 APR 2018

Accepted article online 4 MAY 2018

Published online 24 AUG 2018

## Drainage from the Critical Zone: Lithologic Controls on the Persistence and Spatial Extent of Wetted Channels during the Summer Dry Season

S. M. Lovill<sup>1</sup> , W. J. Hahm<sup>1</sup>, and W. E. Dietrich<sup>1</sup>

<sup>1</sup>Earth and Planetary Science, University of California, Berkeley, CA, USA

**Abstract** In seasonally dry environments, critical zone drainage provides base flow that sustains river ecosystems. The extent of wetted channels and magnitude of base flow throughout the network, however, are rarely documented, and no general theory currently exists enabling the prediction of these key ecosystem properties. We conducted channel surveys in early and late summers of 2012, 2014, and 2015 in four headwater drainage networks (2.8–17.0 km<sup>2</sup>, in the Franciscan Formation of the Eel River (Northern California)), two of which are underlain by the Coastal Belt (argillite and inter-bedded sandstone) and two of which are underlain by the Central Belt (sheared argillaceous-matrix, meta-sedimentary mélange). In all networks, stationary springs controlled the extent of flow. Though surveyed during a period of multiyear drought, the two adjacent Coastal Belt networks remained flowing throughout late-summer months, sustained by drainage from groundwater stored in thick weathered bedrock above fresh, impermeable bedrock. Flow magnitudes, however, decreased and surface flows became increasingly discontinuous, largely due to infiltration into thick gravel deposits on the channel bed. Only 23 km away, in the Central Belt mélange, channel flow ceased early in the summer because the thin critical zone (typically <3 m) stored little water. All late-summer flowing water initiated from deep-rooted sandstone blocks and terminated a short distance down-slope. Our findings suggest that lithology and critical zone development exert primary controls on wetted channel extent. Given similar annual precipitation, nearby watersheds can have dramatically different summer wetted channel networks that result in fundamentally different aquatic ecosystems.

### 1. Introduction

During the extended periods without precipitation that are typical of seasonally dry environments, stream flow inevitably declines, and the extent and persistence of wetted channels in a watershed determine the function and survival of the aquatic ecosystem, as well as surface water resources for terrestrial life. The flow magnitude in wetted channels strongly influences stream temperature (e.g., Webb et al., 2003), aquatic food webs (e.g., Lake, 2003; Larned et al., 2010; Power et al. 2008), habitat availability (e.g., Malard et al., 2006; McKee et al., 2015), and overall water quality (e.g., Wigington et al., 2005). Water temperature strongly controls stream biota survival (e.g., Ray et al., 2012), and transiently wetted channel stretches create gaps that trap and isolate aquatic species that lack the ability to survive in the hyporheic zone (e.g., Jaeger et al., 2014). Fluctuations in water temperature and wetted channel network (WCN) extent affect the habitat connectivity and health of salmonid species, including steelhead (*Onchorhynchus mykiss*) and coho (*Onchorhynchus kisutch*) (e.g., Danehy et al., 2017; Kelson et al., 2016; Schaaf et al., 2017). Furthermore, transiently wetted stretches can produce hypoxic backwater events that can be devastating for certain populations (e.g., Hladzic et al., 2011). Temporary or intermittent streams are beginning to be recognized as a unique ecohydrological type rather than a second-class ecosystem (e.g., Acuña et al., 2017).

Increasingly, there is a need to connect the fate of summer stream flow to land use practices (e.g., Price et al., 2011; Reed et al., 2011; Strauch et al., 2013; Sun et al., 2015; Weitzell et al., 2016), including water extraction (e.g., Arroita et al., 2017), as well as anticipated climate change (e.g., Asarian & Walker, 2016). In the Northern California Coast Ranges specifically, rapid expansion of cannabis cultivation is putting extreme pressure on summer water resources (e.g., Bauer et al., 2015). As a result, springs are being exploited and wetted channels are at heightened risk. At present, we lack observation and theory to mitigate the ecological and societal impacts of these land use changes.

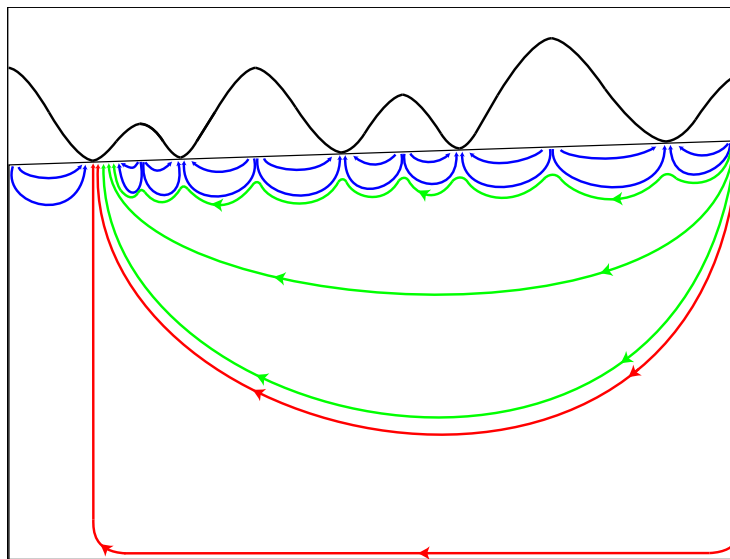


**Figure 1.** Flow simulation of a theoretical aquifer developed in homogeneous lithology (after Tóth, 1963). Flow cells develop as a result of surface topography. Local flow develops in near-surface cells, intermediate flow develops below, and regional flow develops at the base of the aquifer. Arrow size is proportional to relative flow rate.

During base flow, headwater streams act as surficial expressions of groundwater conditions, providing observable spatiotemporal information of groundwater storage within catchments (e.g., Bencala et al., 2011; Biswal & Nagesh Kumar, 2013; Godsey & Kirchner, 2014; Kirchner, 2009; Shaw et al., 2017; Whiting & Godsey, 2016). In rain-dominated climates, all stream flow during these dry periods must come from water stored belowground, typically in the form of slowly draining groundwater that is locally sourced from adjacent hillslopes or is derived from regional groundwater systems that may cross local hillslopes or topographic watershed divides (e.g., Broda et al., 2012, 2014; Clark et al., 2009; Frisbee et al., 2016; Gleeson & Manning, 2008; McNamara et al., 2011; Payn et al., 2012; Sheets et al., 2015; Tague & Grant, 2004; Tóth, 1963; Troch et al., 2003; Welch & Allen, 2012). The hydraulic conductivity, geometry, and volume of this storage source should impact both the persistence and distribution of wetted channels in the dry season.

Figure 1 illustrates Tóth's classical groundwater flow model for complex surface topography, focusing on the general solution for which local topography plays a part in controlling groundwater flow. Local groundwater flow takes place in the near-surface, driven by subtle topographic gradients. Intermediate flow occurs deeper and can cross subtle topographic divides. Regional flow occurs at substantial depths, flowing from a basin's highest point to its lowest point, capable of crossing more prominent topographic divides.

In contrast, hydrologic studies of the critical zone (from canopy top to fresh bedrock) under hillslopes suggest that wet season groundwater storage may develop above the fresh bedrock and slowly drain to channels, maintaining base flow (e.g., Anderson et al., 2002; Rempe & Dietrich, 2014, 2018; Salve et al., 2012). Here, the groundwater entering streams is locally derived from the adjacent hillslope and is not part of a larger aquifer of the kind conceived in the Tóth models. Studies of the subsurface critical zone have found that the thickness tends to vary systematically across hillslope profiles (e.g., Holbrook et al., 2014; Lebedeva & Brantley, 2013; Rempe & Dietrich, 2014; Riebe et al., 2017; St. Clair et al., 2015), influencing the dry season drainage that sustains the wetted channel network.

The thickness of alluvial fill in the channel bed also affects the distribution of wetted channels. Conductive, in-channel sediment fill that lines the channel can cause streamflow to go subsurface during low flows (hyporheic flow; e.g., Godsey & Kirchner, 2014; Queener & Stubblefield, 2016; Whiting & Godsey, 2016). At present, however, we generally lack field data on the occurrence of sediment fill and its impact on the extent and magnitude of flow in wetted channels during dry periods.

Recent wetted channel mapping efforts have targeted watersheds over seasonal time scales. Godsey and Kirchner (2014) mapped seasonal wetted channel dynamics in California headwater catchments of various

sizes ( $4.0\text{--}27.2 \text{ km}^2$ ) and geologic settings, relating power-law functions of runoff to WCN lengths. They noted the location of “flowing channel heads” (referred to as “flowheads” in our study), where each flowing channel initiates. In the surveyed networks, they observed seasonally variable flowhead locations, and disconnection and subsequent reconnection of WCNs (wetted channels were “disconnected” by dry channel segments and became “reconnected” downstream, where channels redeveloped flow) that contributed to dynamic drainage networks. Their WCN lengths fluctuated substantially with changes in runoff (which

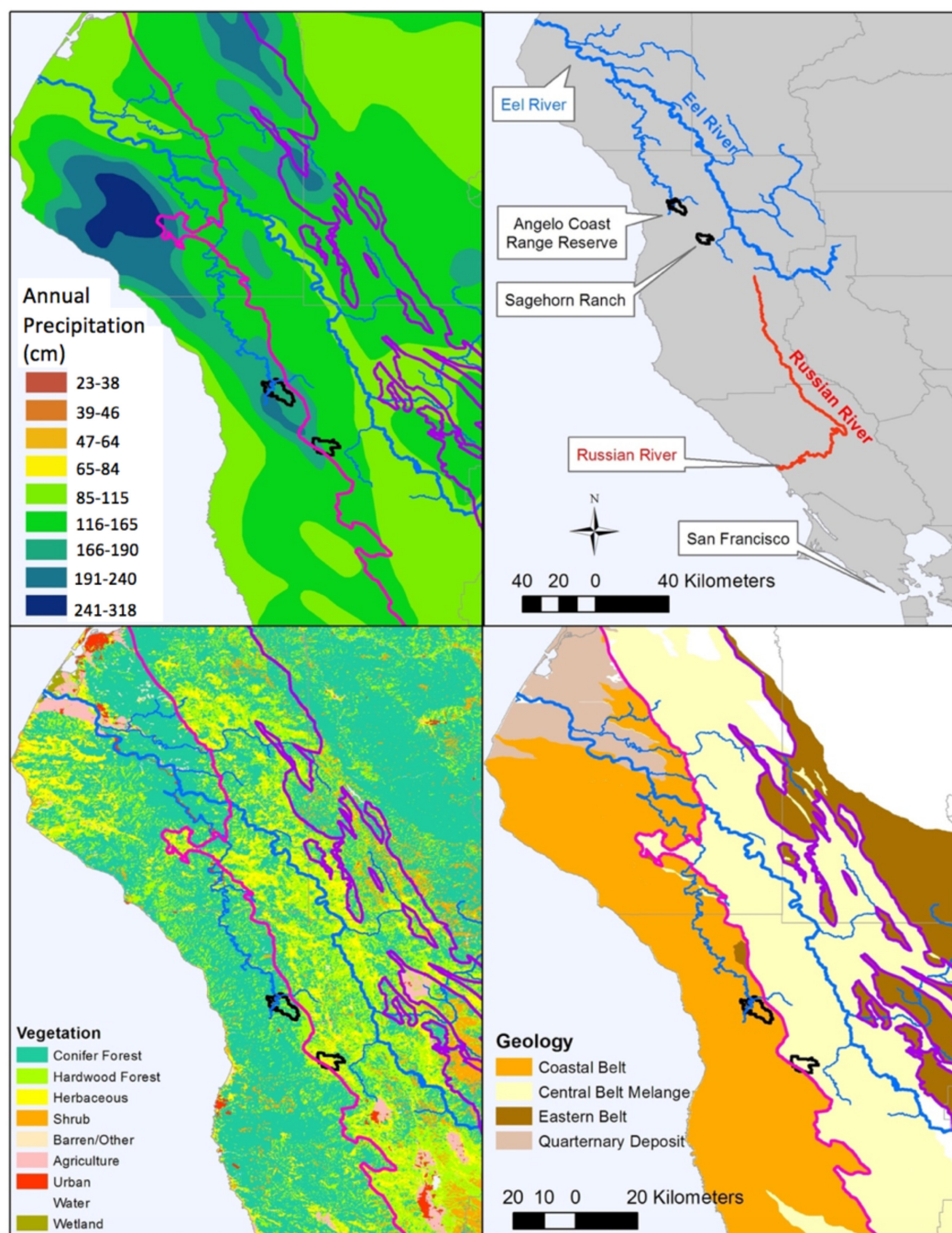


**Figure 2.** Climatic, vegetation, and geologic setting of the two field sites (black outline): Angelo Coast Range Reserve (northern) and Sagehorn Ranch (southern). Annual precipitation is derived from Cal-Atlas Geospatial Clearinghouse (mean from 1900 to 1960). Vegetation is derived from the California Resources Agency, Legacy Project (2003). Geology is derived from McLaughlin et al. (2000). Note geologic boundaries are present on vegetation map.

ranged from 0.05 to 4.08 mm/d). Whiting and Godsey (2016) documented WCN-runoff relationships in headwater catchments in Central Idaho ( $6.5\text{--}21.4 \text{ km}^2$ ) over the course of the 2014 spring and summer. In contrast to Godsey and Kirchner (2014), they observed mostly stationary flowheads (i.e., flowheads remaining in the same location throughout all surveys) despite runoff ranging from 0.08 to 2.21 mm/d, with accordingly little variation in the WCN. Our analysis of their data suggests that in these Idaho watersheds, an average of 55% of the decrease in the WCN, associated with declining discharge, could be attributed to disconnections in the WCN. In a  $1.5 \text{ km}^2$  New York state headwater catchment, Shaw (2016) observed seasonally stationary flowheads, with changes in the WCN also primarily controlled by disconnections in the network downstream of flowheads. Zimmer and McGlynn (2017) focused on runoff generation processes in a small ( $0.03 \text{ km}^2$ ), low-slope watershed, and observed variable flowhead position, often upslope of geomorphic channel heads in response to storm events. Remote sensing technology has recently been used to map wetted channels in larger watersheds in nonvegetated environments, using high-resolution multispectral band analysis (e.g., Hamada et al., 2016), LiDAR (e.g., Liu et al., 2017), and digital aerial orthophotographs (e.g., Persendt & Gomez, 2016). Additional work has used a combination of orthophotographs and on-ground mapping (e.g., González-Ferreras & Barquín, 2017) to quantify the ubiquitous underrepresentation of ephemeral channels, and to illuminate their importance, both ecologically and hydrologically.

These studies reveal four important attributes of wetted channels: (1) flowhead position (stationary or variable); (2) wetted channel drainage density; (3) the length of wetted channels that are continuously connected, relative to the length of the WCN; and (4) stream discharge, measured in reaches with little to no sediment fill, downstream of surveyed WCNs. Godsey and Kirchner (2014) and Whiting and Godsey (2016) suggest that disconnections in the WCN are driven by hyporheic flow through conductive sediment, and explore fundamental causes for the variable and nearly invariant WCN lengths in their respective studies. However, neither study offers further explanation as to what might control absolute WCN length. We propose that these differences can be explained through the lens of critical zone structure and dynamics.

Here we take advantage of the Eel River Critical Zone Observatory (ERCZO), in the Northern California Coast Ranges, to map summer wetted channel extent in two nearby locations (see Figure 2). These sites experience a similar Mediterranean climate, but their underlying lithology and critical zone structures are radically different. One site (Angelo Coast Range Reserve), in the Coastal Belt argillite and sandstone, has a deep, water-storing critical zone with a thick unsaturated zone (Salve et al., 2012). The other site (Sagehorn), in the Central Belt mélange, has a shallow, low-storage critical zone with a thin unsaturated zone (Hahm et al., 2016; Rempe et al., 2015). By coupling our understanding of the subsurface hydrology of our sites (Dralle et al., 2016; Druhan et al., 2017; Hahm et al., 2016, 2017; Kim et al., 2017; Link et al., 2014; Oshun et al., 2016; Rempe & Dietrich, 2014; Rempe et al., 2010; Salve et al., 2012) with wetted channel observations at the beginning and end of the summer dry season, our study demonstrates the connection between critical zone structure and the extent and duration of wetted channels.

Our analysis proceeds by first describing each field site, making specific links between lithology, critical zone structure, and the hydrologic processes that dictate summer base flow controlling wetted channel distribution. We then quantify the geomorphic channel network structure for each site to define the context and possible influence on the dry season wetted channel network. Results of extensive mapping of wetted channels and flowhead locations at the start and near the end of dry season reveal the influence of lithology, critical zone structure, and geomorphic channel network structure on the spatial extent and density of wetted channels through the summer dry season.

## 2. Site Descriptions

### 2.1. Northern California Coast Ranges Geomorphic Context

The northward-propagating crustal thickening and uplift, associated with the northward passage of the Mendocino triple junction (MTJ), has generated waves of uplift that swept through the region in the past few million years (e.g., Mackey et al., 2014; Lock et al., 2006; Willenbring et al., 2013), and raised our study sites above sea level. This is reflected by northwest trending ridges and axial drainages and has forced migrating knickpoints, river capture, and drainage reversals, generating “fish hook” drainage patterns in several Eel River tributaries (Bennett et al., 2016; Lock et al., 2006; Roering et al., 2015; Willenbring et al., 2013). Pulses of incision likely also originated from sediment supply reduction from the Pleistocene to the

Holocene (Fuller et al., 2009), as well as bedrock meander cutoffs that generated upstream migrating knickpoints (Finnegan & Dietrich, 2011). Knickpoints are present along the river networks of both of our study sites.

### 2.1.1. Angelo

We mapped the wetted channel network in Elder and Fox Creek watersheds (Figure 3), which lie in the Angelo Coast Range Reserve (Angelo). The area experiences a Mediterranean climate, with cool, wet (rain-dominated) winters and warm, dry summers. Using PRISM data, Angelo average annual precipitation and temperature from 1981 to 2010 was 2042 mm and 12.4°C, respectively (PRISM, 2010). In 2012 and 2014 surveys were conducted at Fox ( $2.75 \text{ km}^2$ ) and Elder ( $16.97 \text{ km}^2$ ), which drain west into the north-flowing South Fork of the Eel River (Figure 3). The study coincided with a period of state-wide drought with precipitation totals of 1,630 mm (2012), 1,447 mm (2013), 1,027 mm (2014), and 1,403 mm (2015) (measured at our Angelo meadow weather station, and not corrected for wind losses). Figures 4a and 4b show summer precipitation, annual fluctuations in Elder discharge, and summer runoff data for the study years compared to all previous years, demonstrating that very little precipitation occurred during the period of survey with no consequences for runoff.

Angelo is underlain by the Coastal Belt, the westernmost part of the Franciscan Formation Complex (e.g., Blake et al., 1988; Dumitru et al., 2010; Langenheim et al., 2013; McLaughlin et al., 2000). The Coastal Belt is composed of a slightly metamorphosed marine turbidite sequence of shales, sandstones, and conglomerates (Ernst, 1970), with paleo-burial depths of less than 5–8 km (Ernst & McLaughlin, 2012). The Fox and Elder watersheds are almost entirely underlain by rocks of the Coastal Belt Yager terrane (Ernst & McLaughlin, 2012), which consists of nearly vertically dipping Paleocene and Eocene argillite and thinly bedded arkosic sandstone with rare conglomerate facies (Langenheim et al., 2013; Underwood, 1983).

Channel incision (0.2–0.4 mm/yr; Fuller et al., 2009) has cut narrow canyons and led to steep hillslopes (watershed average slope for 1 m pixels is 51%) prone to deep-seated landslides and shallow debris flows. Debris flow deposits are found in the fans at the tributary junctions to Elder and in many parts of Fox Creek.

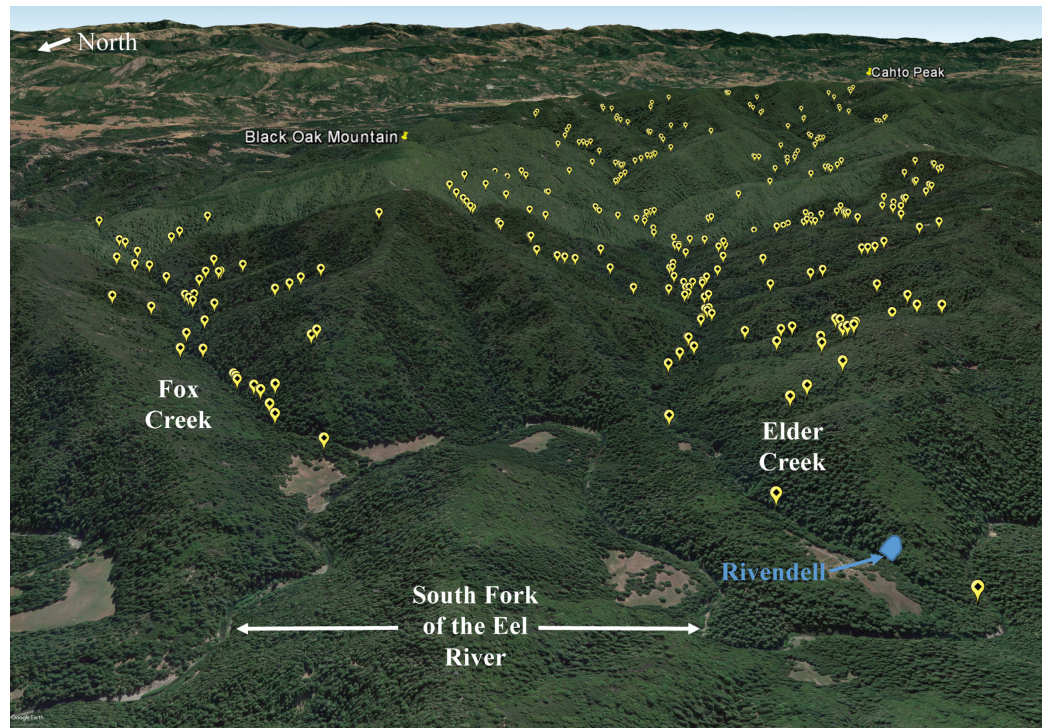


**Figure 3.** Angelo early summer 2014 location of data collection points (yellow markers), taken in channels and at flow-heads. Shown on a Google Earth image of Fox and Elder Creek watersheds. Note location of Rivendell (bottom right), the South Fork of the Eel River (bottom) Black Oak Mountain (top middle), and Cahto Peak (top right).

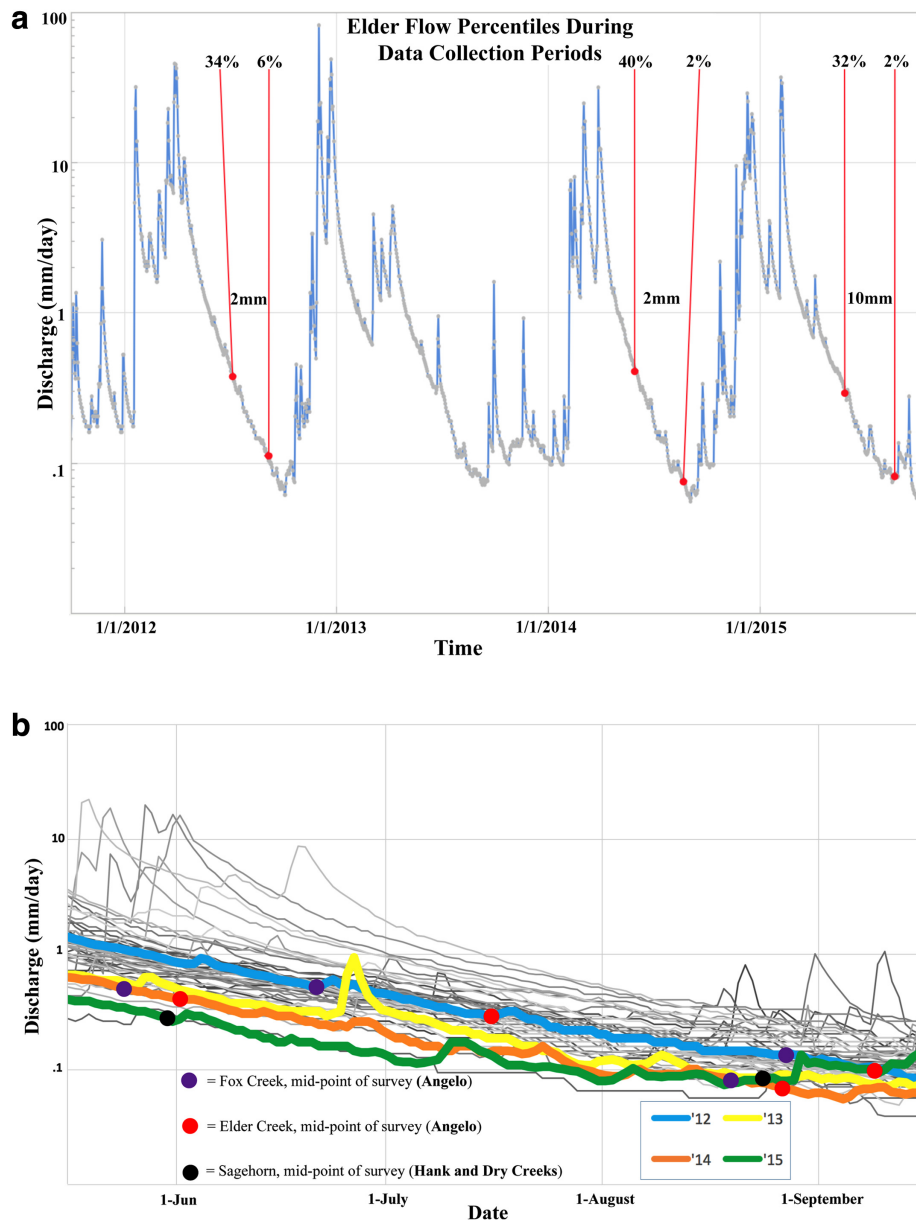


**Figure 4.** (a) Annual Elder daily discharge fluctuations, during survey years. Red dots are the midpoint of each survey period. The percent of time flow has spent at or below that value from 1967 to 2015 at the midpoint of the survey period is indicated by black numbers above red line segments. Total precipitation recorded at Angelo Meadow weather station in between wetted channel survey periods is reported in millimeter values in between red line segments. (b) Elder Creek summer discharge from 16 May to 15 September (1968–2015). Years 1968–2011 are thin, grayscale lines while the years 2012–2015 are bold, and color-coded (legend gives years). The timing and discharge at the midpoint of each survey on each year's discharge line are indicated by purple (Fox), red (Elder), and black (Hank and Dry Creeks) circles. Dry and Hank creeks were surveyed concurrently, so one data point sufficiently represents the midpoint of each survey for both watersheds.

Old-growth forest extends across Angelo. South-facing slopes are dominated by hardwoods, mainly Pacific madrone (*Arbutus menziesii*), interior live oak (*Quercus wislizenii*), California black oak (*Quercus kelloggii*), canyon live oak (*Quercus chrysolepis*), and California bay laurel (*Umbellularia californica*), with lesser tanoak (*Notholithocarpus densiflorus*), Pacific yew (*Taxus brevifolia*), and chinquapin (*Castanopsis chrysophylla*). On south-facing slopes, mature Douglas firs (*Pseudotsuga menziesii*) are primarily present in canyon bottoms, and extend upslope only in moist regions, but young Douglas fir understory can be found throughout. North-facing slopes are predominately inhabited by Douglas firs, tanoaks, and to a lesser extent, the afore-

mentioned hardwood species. The current mosaic of Douglas fir and hardwood species appears to be a legacy of native American fire practices, followed by fire suppression in the past century (Johnson, 1979).

As part of the Eel River Critical Zone Observatory in Angelo, an intensively monitored site, Rivendell, was established on a hillslope near the mouth of Elder Creek (Salve et al., 2012). It is mostly underlain by argillite. Here, thin, porous soils (10–70 cm thick) lie above a 2–4 m layer of saprolite (Oshun et al., 2016; Salve et al., 2012). Weathered bedrock below this saprolite is mechanically harder, and shows signs of mechanical and chemical alteration (oxidation), with opened interconnected fractures that provide flow paths for runoff generation (Oshun et al., 2016; Rempe, 2016; Salve et al., 2012). This weathered bedrock layer thickens toward the divide, and decreases in fracture intensity and degree of weathering with depth (Salve et al., 2012). The depth to fresh bedrock varies from 4 m at the toe of the hillslope to 25 m at the ridge, 150 m above Elder Creek (Rempe et al., 2010; Rempe & Dietrich, 2014). Shallow seismic surveys at four other nearby hillslopes indicate that the topographic variation in critical zone thickness is similar to that found at Rivendell (Rempe et al., 2015).

At Rivendell, data on groundwater table levels, groundwater and stream water chemistry, soil and rock moisture, water isotope dynamics, meteorology, sap flow, subsurface temperature and CO<sub>2</sub> have been continuously collected, with a principal focus of understanding the path and solute evolution of water through the critical zone (Druhan et al., 2017; Kim et al., 2014, 2017; Link et al., 2014; Oshun et al., 2016; Rempe, 2016, Rempe & Dietrich, 2014, 2018; Salve et al., 2012). At the start of the wet season, most of the infiltrating rain increases the moisture content in the soil and the underlying weathered bedrock. As the wet season continues, the rock moisture (in the sense of, Rempe & Dietrich, 2018; Salve et al., 2012) increases until the total storage increase is about 100–550 mm depending on position along the hillslope (Rempe, 2016; Rempe & Dietrich, 2018), beyond which additional fracture flow to groundwater develops above the fresh bedrock boundary. Groundwater levels rise and fall with most major storms. Incoming precipitation travels through the unsaturated zone to the groundwater, where it drains laterally via fractures to the channel. Saturation overland flow occurs only in unchanneled valleys during extended periods of intense rainfall. At the end of the wet season, the groundwater declines rapidly at first and then progressively more slowly through the dry season. It is this slow drainage, travelling as fracture flow and emerging at springs, that supports the wetted channels of Elder Creek.

We assume the critical zone structure, observed in the Rivendell hillslope (and noted through geophysical surveys elsewhere in the Angelo), applies throughout the Fox and Elder watersheds. Field observations indicate that thick sandstone interbeds typically outcrop and likely have different critical zone structure. However, at Angelo these interbeds make up a smaller component of the bedrock (less than 35%) and generally are not thick enough to dominate entire hillslopes.

### 2.1.2. Sagehorn

The 2015 surveys concentrated on the Dry and Hank drainages, with areas of 3.54 and 5.59 km<sup>2</sup>, respectively (Figure 5). These watersheds are located on the Sagehorn-Russell Ranch (referred to as Sagehorn throughout this study), a 21.1 km<sup>2</sup>, privately owned, lightly grazed cattle ranch 23 km SSE of Rivendell (Figures 2 and 5). Sagehorn receives slightly less precipitation than Angelo, but due to greater canopy interception at Angelo effective precipitation is comparable (Hahm et al., 2017; Rantz, 1968). As in Angelo, most of the precipitation falls as rain, but occasional storms produce snowfall. Annual average temperature at Sagehorn is 13.3°C (0.9°C higher annually than Angelo, PRISM, 2010).

Sagehorn lies within the Central Belt of the Franciscan Complex, which consists of subduction-zone-related bedrock from the accretionary prism that developed 88–40 Ma ago, as the Farallon Plate subducted beneath North America, prior to emplacement of the Coastal Belt (McLaughlin et al., 2000). The Central Belt consists of an extensive argillaceous mélange, and is noted for its large volume of shale matrix (Cloos, 1982). In this mélange, more coherent blocks ranging from sand-sized particles to mountains (10<sup>-2</sup> to 10<sup>4</sup> m) (Roering et al., 2015) are encased in a heavily deformed, weak, fine-grained, argillic matrix. These blocks include sandstone, shale, greenstone, chert/metachert with a small volume (< 1%) of exotic blocks of blue schist and rare amphibolite and eclogite (Ukar & Cloos, 2016).

The larger, more competent blocks manifest as topographic highs amid the mélange matrix (e.g., Roering et al., 2015). Earthflow topography is widespread on hillslopes, which are not as steep as Angelo (generally less than 30%). However, currently no earthflows are visibly active in either Dry or Hank Creek watersheds.

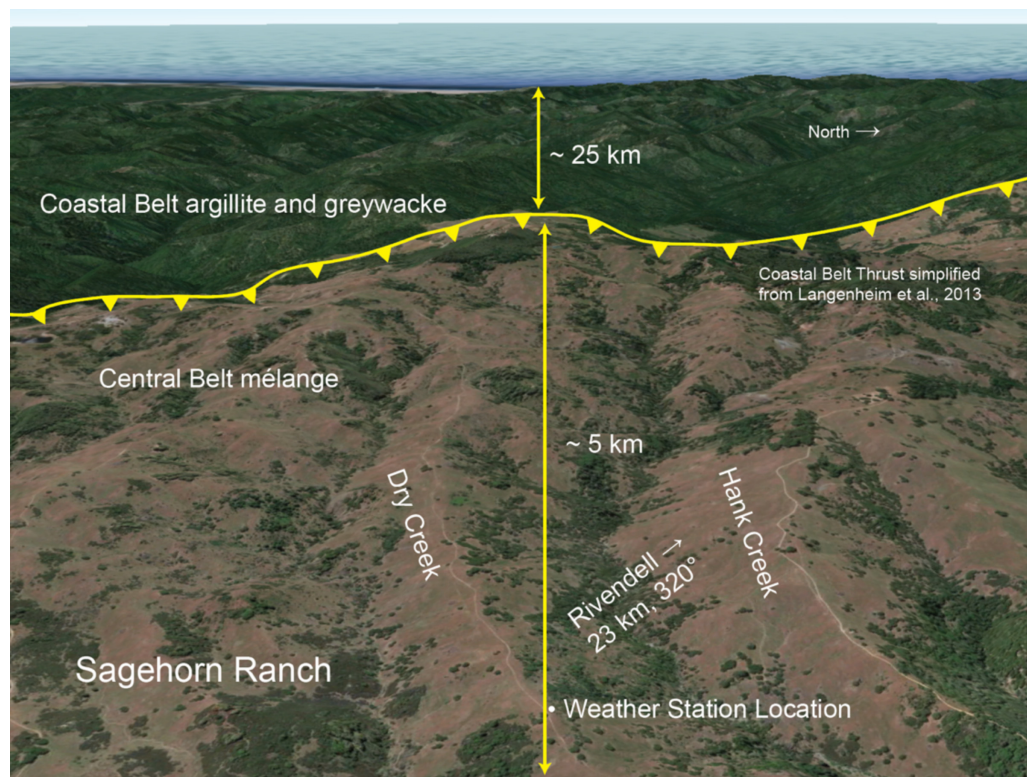


**Figure 5.** The Dry and Hank Creek watersheds on the Sagehorn Ranch. Image looks due west toward the Pacific Ocean. The thrust boundary (yellow line) lies between the Coastal Belt to the west and Central Belt in the east. Patches of forests in the Central Belt mostly correspond to sandstone blocks in the mélange. Rivendell, Elder, and Fox are located 23 km to the NNW.

Sagehorn is a sparsely forested savanna-woodland (28.3% canopy cover). Approximately 90% of the grasses in Sagehorn are now invasive annuals. Water-limitation tolerant Oregon White Oaks (*Quercus garryana*) are the dominant tree on the mélange matrix (Hahm et al., 2017; Hahm et al., 2018). Trees primarily growing on sandstone blocks include California black oak, California buckeye, Douglas fir, California bay laurel, Pacific madrone, and tanoak.

Extensive drilling and hydrologic monitoring at Sagehorn has shown that only a shallow critical zone (typically less than 3 m) has developed over fresh, unoxidized bedrock (Hahm et al., 2016). In 2014 and 2015 drilling on the divide between Hank and Dry in the driest month after extensive drought, the fresh bedrock was saturated even though it lay just few meters below the surface. Hence, the groundwater in the fresh bedrock is essentially stagnant. In contrast, winter rainfall infiltrates through the weathered bedrock of the critical zone and ponds on the saturated fresh bedrock, forming a dynamic saturated zone that fluctuates near the ground surface over the winter and early spring months, as it is recharged during individual storm events, and subsequently drained during dry periods (Hahm et al., 2017; Dralle et al., 2018). Larger rainfall events cause the water table to rise to the surface, generating saturation overland flow across the entire landscape. This runoff collects and rapidly flows down a relatively dense channel network (see below) to Hank and Dry Creek (Hahm et al., 2017). The groundwater table falls after the end of the rainy season due to evaporation, water used by vegetation, and some lateral drainage. Essentially no water arrives from the mélange at Hank and Dry creek in the summer (Hahm et al., 2017).

### 3. Methods

Channel surveys were conducted in early and late summer in Fox and Elder Creeks (Coastal Belt) in 2012 (over 17 days in the early summer and 10 days in the late summer) and 2014 (over 14 days in the early summer and 12 days in the late summer). In each survey, the entire wetted channel network was walked and

mapped, requiring 200–250 km of hiking through rugged terrain (Figure 3). In 2015, (over 5 days in the early summer and 5 days in the late summer) the Dry and Hank watersheds in the Central Belt mélange were surveyed, but some stretches of channel were overlooked, due to low-precision contour maps, and insufficient mapping. These channel stretches were revisited at similar time periods during the summer of 2016 with higher resolution lidar-based maps. The 2015 surveys in Sagehorn each required 100–150 km of hiking.

Surveys were performed by hiking every tributary and subtributary of each watershed, while continuously mapping the presence or absence of surface flow. This was accomplished by regularly noting topographic features in order to identify location on the 1 m contour maps (derived by LiDAR, courtesy of the National Center for Airborne Laser Mapping) in order to most accurately mark the transition between wet and dry channels. Flow was followed to its upstream origin within each subdrainage to map the location of flowheads. We defined flowheads as the highest elevation location within each subdrainage area, where flow initiated at the time of the survey. Sites where flow re-emerged from a dry channel, downslope of a flowing stretch, were not considered flowheads.

In total, over 1,100 sites were catalogued over the course of the study. At each site, GPS location was recorded, though the positioning in high-sloped heavily forested locations had a poor accuracy (up to 30 horizontal meters). The location by eye of the observation point on the LiDAR map was commonly far more accurate (Figure 3 shows the location of data points in the Fox and Elder Creek watersheds). At each site, channel width, depth, water temperature, air temperature, air humidity, and additional data types (Lovill, 2016) were recorded, and water isotope samples were collected to help decipher how water sources changed over the summer months. Data were collected in the early summer ("Round 1"), and then late summer ("Round 2") at the exact same location (by using photographs of early summer data point locations in the field during late summer surveys) to compare how hydrological and environmental characteristics had changed.

All data were digitized and georeferenced, and all numerical data not collected in the field (i.e., drainage area, slope, elevation, geomorphic channel drainage densities, and wetted channel drainage densities (WCDDs)) were derived, using ArcGIS (applying the D-8 steepest flow path slope algorithm) in conjunction with raster analysis in Python. WCDDs were calculated by translating hand-drawn wetted segments on field maps to ArcGIS, summing all wetted segments within each watershed downstream of geomorphic channel heads, and then dividing by watershed drainage area.

We constructed maps of the geomorphic channel network for the Fox (Coastal Belt) and Dry (Central Belt) watersheds. We define the geomorphic channels in the field by the presence of banks (Dietrich & Dunne, 1993). Field mapping confirmed that geomorphic channels can readily be identified with contours gridded from 1 m horizontal pixel resolution, lidar-derived digital elevation via the indentation of contour lines. The channel head commonly occurs where contours switch from predominantly U-shaped (smooth hillslopes) to V-shaped (incised channels).

We then determined the drainage area to initiate channel heads, observed in the field, for the Fox (initiation area = 6,180 m<sup>2</sup>) and Dry (1,085 m<sup>2</sup>) watersheds. The average drainage areas for each watershed, which differed significantly, were subsequently applied to corresponding adjacent watersheds, Elder and Hank, to define channel initiation points and thus the geomorphic channel network in those watersheds. There was generally good correspondence between mapped location of channel heads, change in contour configuration from U to V shaped, and the location of the channel heads, predicted from the mean threshold area.

Using standard algorithms in ArcGIS, we calculated flow direction (D8), flow accumulation and flow lengths using a 1 m bare-earth lidar raster. We then extracted all points with drainage areas above our geomorphic channel threshold, and plotted their elevation versus flow length to create the channel long profile maps.

Discharge in the Fox Creek watershed is not monitored, so Elder Creek's unit area runoff (calculated from Elder discharge at the USGS gaging station) was used to estimate Fox Creek discharge. Stream flow monitoring in Dry Creek was initiated in November 2015 (after our Sagehorn surveys) but there was no continuous flow in either Dry or Hank creeks during the summer study window. Periodic gaging has been conducted on Hank and Dry creeks, using a hand-held acoustic Doppler velocimeter (Sontek) to establish rating curves.

More details about methods and errors related to wetted channel lengths for all surveys can be found in Lovill (2016).

## 4. Results

### 4.1. Channel Networks in a Watershed Setting

All summer wetted channels lie within the geomorphic channel network, hence it is useful to quantify the geomorphic channel network as a framework for understanding the extent of wetted channels. This geomorphic channel network analysis indicates striking differences in steepness, sediment cover, and drainage density between the two lithologies. The mean gradient (average slope of all 1 m<sup>2</sup> pixels) in the Fox and Elder watersheds (51.3% and 50.4%, respectively (50.6% area-weighted combination)) is much greater than that of the Hank and Dry Creek watersheds, in Sagehorn, (30.2% and 27.9% for Hank and Dry, respectively, and 28.8% combined). Figure 6 shows the longitudinal profile of all geomorphic channels (both dry and wetted) for each surveyed basin and supporting information Figure S.1 shows the reach-scale channel gradient for the four watersheds. Figure 7 combines all the data into a single plot of slope versus drainage area for the channel network. Channel topographic characteristics of adjacent creeks in the same lithology are remarkably similar, but differ greatly within nearby channel networks of different lithology.

In Elder, the first 4.5 km upstream from the mouth has a low, increasing slope (from about 2.4%–3.1%) and is marked, as Seidl and Dietrich (1992) noted, by two local knickpoints (at 2.3 and 3 km upstream). The knickpoint at 2.3 km has about a 7 m local elevation step, whereas the upper knickpoint is shallower and less distinct. Seidl and Dietrich (1992) interpreted the knickpoints as recording upstream propagating steps, and subsequent dating of strath terraces by Fuller et al. (2009) indicates that these knickpoints are associated with Holocene channel incision. Further upstream the main stem steepens, eventually averaging 20%

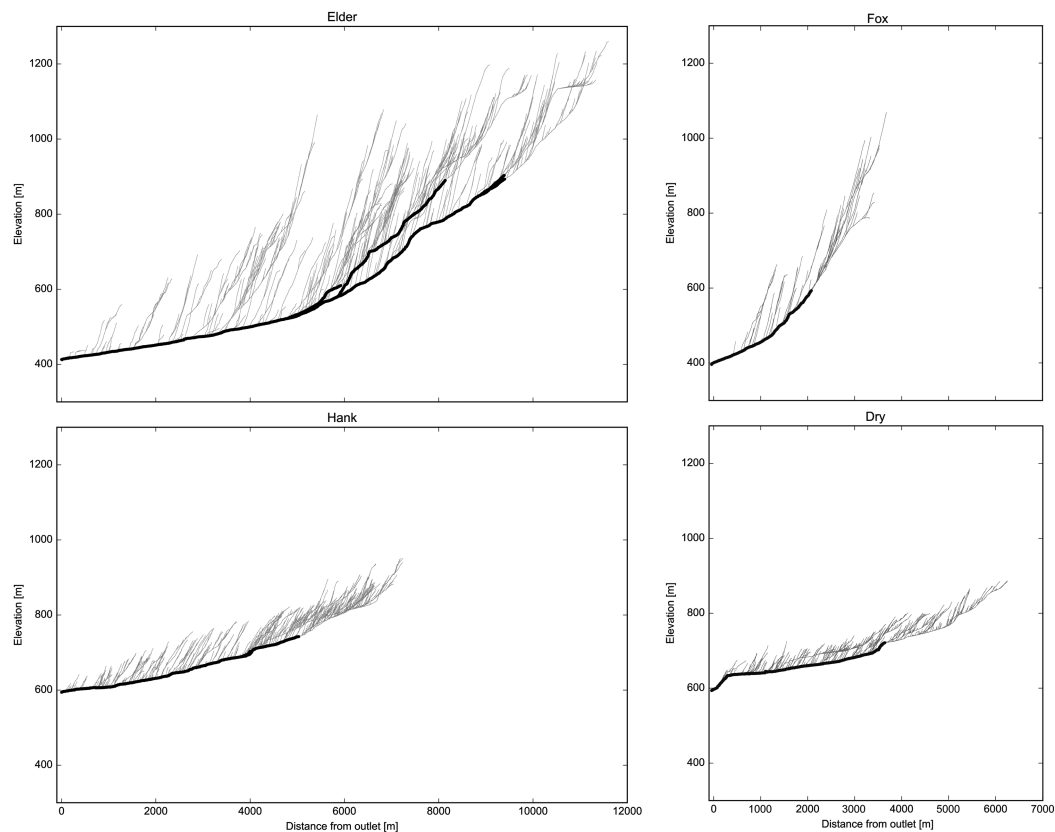


**Figure 6.** Longitudinal profiles for all geomorphic channels within each surveyed watershed. Profiles are shown for Elder, Hank, Fox, and Dry Creek. Channel networks in the Coastal Belt (Elder and Fox) are much steeper than those of the Central Belt (Hank and Dry). The overall relief in the watersheds is also greater in the Coastal Belt. The longitudinal profiles for each watershed have the same horizontal and vertical scale to aid in network comparison. The channel network in each profile was derived from drainage area thresholds of 6,180 m<sup>2</sup> for the Fox and Elder creek watersheds and 1,085 m<sup>2</sup> for the Hank and Dry Creek watersheds. Channels with drainage areas greater than 1 km<sup>2</sup> are bolded for the distinction of main stems from the rest of the network. Fox and Dry longitudinal profiles have smaller drainage areas compared to Elder and Hank and therefore have shorter distances from headwaters to mouths. These profiles have the same scale and are included to the right for comparison.

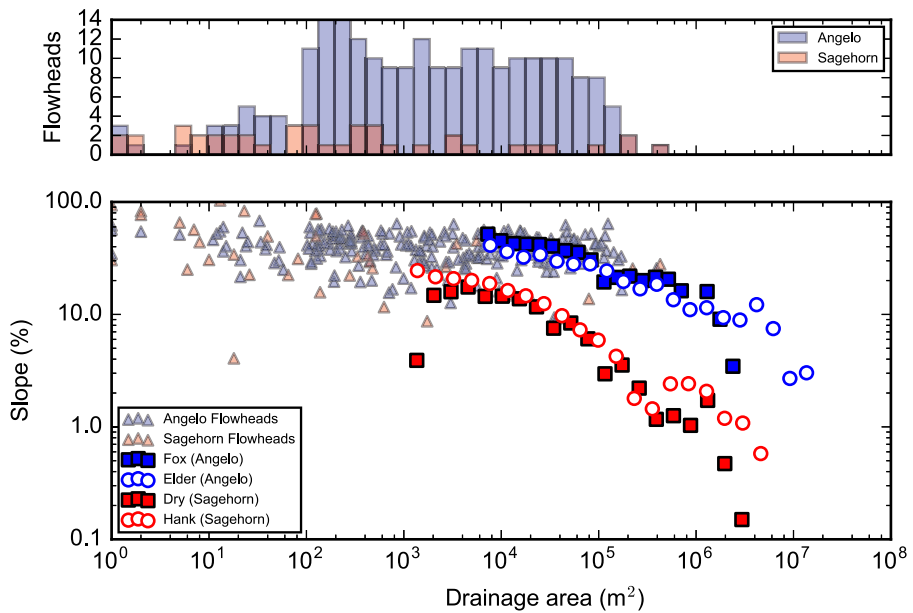


**Figure 7.** Local slope versus drainage area along the geomorphic channel network in the Fox, Elder, Dry, and Hank watersheds, and drainage area to flowheads for the two watersheds in Angelo and Sagehorn. Data points are color coded by watershed. All 2014 and 2015 flowheads, collected in the field are represented by transparent triangles, outlined in black, and are shown in the histogram above the plot, and all squares and circles represent the average slope (binned by drainage area) along the main stem of respective channel networks. The histogram and the plot both show that flowhead drainage areas span 6 orders of magnitude in both Angelo and Sagehorn.

for the final nearly 3 km and is covered in coarse sediment. The tributaries entering Elder are steep (Figure 6), bouldery, and at the tributary junctions, there are distinct fans constructed from successive debris flow deposits, derived from the tributary outflows (Scheingross, et al., 2013; Seidl & Dietrich, 1992). The supporting information provides more detailed discussion related to the geomorphic properties and processes acting on the Fox, Hank, and Dry Creek channel networks. The supporting information also reviews process controls on the river profiles, as proposed by Sklar and Dietrich (2004, 2008), Stock and Dietrich (2003, 2006), and Stock et al. (2005).

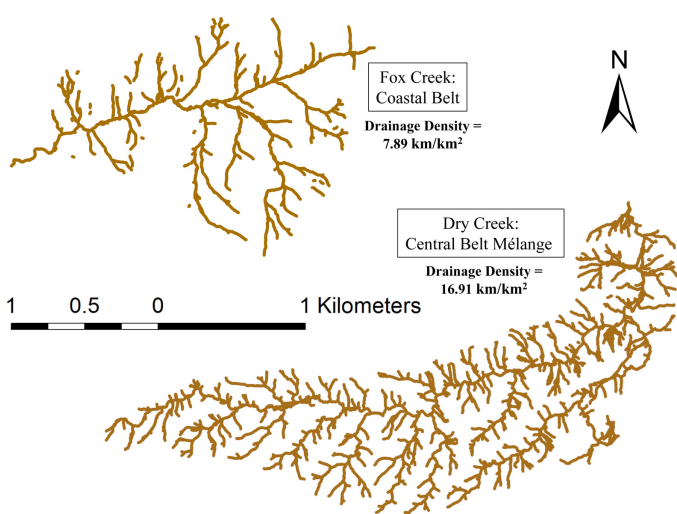


**Figure 8.** Drainage density comparison of Fox and Dry Creek geomorphic channel networks. Dry Creek watershed developed in Central Belt has over twice the channelized drainage density of the Fox Creek watershed (part of the Coastal Belt in Angelo).

Figure 8 shows the mapped channel network for Fox and Dry, revealing that the drainage density of geomorphic channels is twice in Dry, relative to Fox. Given that overland flow extends across the entire landscape, relatively small drainage areas (leading to relatively large drainage densities) may be required to generate the shear stress necessary to mobilize the fine sediment of the mélange matrix.

Figure 7 shows that the local slope and drainage area of the channel network within the same lithology is nearly identical for adjacent watersheds, but is very different between lithologies. We interpret the Coastal Belt slope-area relationship to represent the dominance of debris flow bedrock incision that dominates even channels draining greater than 1 km $^2$  (as field observations indicate). In the Central Belt, fluvial bedrock incision and sediment transport extends through most, if not the entire channel network.

#### 4.2. Angelo Coastal Range Reserve Results

##### 4.2.1. Similarities in Adjacent Watershed Wetted Channel Drainage Densities (WCDDs)

In the early summer of 2014, the 2.75 km $^2$  Fox Creek and the 17.0 km $^2$  Elder Creek in the Coastal Belt exhibited nearly identical WCDDs of 1.95 and 1.93 km/km $^2$ , respectively (Table 1). The early summer

**Table 1**

*Watershed, Wetted Channel, and Flowhead Characteristics for All Field Surveys*

| Year & round #            | Watershed | Dates     | Watershed drainage area (km <sup>2</sup> ) | drainage density (km/km <sup>2</sup> ) | <sup>c</sup> WCDD (km/km <sup>2</sup> ) | Wetted channel length (km) | Continuous WCDD (km/km <sup>2</sup> ) | Continuous wetted channel length (km) | Elder creek discharge during survey (mm/d) | Elder creek flow percentile during survey (%) | Total # of flowheads | % of round 2 retractions |
|---------------------------|-----------|-----------|--|--|---|----------------------------|---------------------------------------|---------------------------------------|--|---|----------------------|--------------------------|
| <sup>b</sup> 2012 Round 1 | Fox       | 6/18–7/3  | 2.75                                       | 7.89                                   | 2.09                                    | 5.74                       | 0.57                                  | 1.55                                  | 0.54                                       | 44.0  | <sup>a</sup> N/A     | <sup>a</sup> N/A         |
| <sup>b</sup> 2012 Round 2 | Fox       | 8/24–8/25 | 2.75                                       | 7.89                                   | 1.52                                    | 4.15                       | 0.50                                  | 1.37                                  | 0.14                                       | 12.6  | <sup>a</sup> N/A     | <sup>a</sup> N/A         |
| <sup>b</sup> 2014 Round 1 | Fox       | 5/23–5/24 | 2.75                                       | 7.89                                   | 1.96                                    | 5.37                       | 0.51                                  | 1.39                                  | 0.51                                       | 43.1  | 33                   | <sup>a</sup> N/A         |
| <sup>b</sup> 2014 Round 2 | Fox       | 8/17–8/18 | 2.75                                       | 7.89                                   | 1.45                                    | 3.97                       | 0.24                                  | 0.66                                  | 0.08                                       | 3.1   | 28                   | 6.1%                     |
| <sup>b</sup> 2012 Round 1 | Elder     | 7/4–7/23  | 16.97                                      | 7.89                                   | 2.01                                    | 34.02                      | 0.77                                  | 13.01                                 | 0.32                                       | 34.2  | <sup>a</sup> N/A     | <sup>a</sup> N/A         |
| <sup>b</sup> 2012 Round 2 | Elder     | 8/26–9/23 | 16.97                                      | 7.89                                   | 1.60                                    | 27.19                      | 0.72                                  | 12.23                                 | 0.1  | 5.7   | <sup>a</sup> N/A     | <sup>a</sup> N/A         |
| <sup>b</sup> 2014 Round 1 | Elder     | 5/25–6/7  | 16.97                                      | 7.89                                   | 1.93                                    | 32.68                      | 0.73                                  | 12.39                                 | 0.42                                       | 39.7  | 195                  | <sup>a</sup> N/A         |
| <sup>b</sup> 2014 Round 2 | Elder     | 8/19–8/28 | 16.97                                      | 7.89                                   | 1.43                                    | 24.31                      | 0.68                                  | 11.51                                 | 0.07                                       | 1.8   | 162                  | 3.6%                     |
| <sup>b</sup> 2015 Round 1 | Dry       | 5/26–6/1  | 3.54                                       | 16.91                                  | 0.86                                    | 3.03                       | 0.00                                  | 0.00                                  | 0.30                                       | 32.2  | 17                   | <sup>a</sup> N/A         |
| <sup>b</sup> 2015 Round 2 | Dry       | 8/20–8/24 | 3.54                                       | 16.91                                  | 0.15                                    | 0.54                       | 0.00                                  | 0.00                                  | 0.08                                       | 2.3   | 12                   | 0%                       |
| <sup>b</sup> 2015 Round 1 | Hank      | 5/26–6/1  | 5.59                                       | 16.91                                  | 1.22                                    | 6.80                       | 0.00                                  | 0.00                                  | 0.30                                       | 32.2  | 26                   | <sup>a</sup> N/A         |
| <sup>b</sup> 2015 Round 2 | Hank      | 8/20–8/24 | 5.59                                       | 16.91                                  | 0.11                                    | 0.63                       | 0.00                                  | 0.00                                  | 0.08                                       | 2.3   | 14                   | 0%                       |

<sup>a</sup>N/A refers to "not available." Flowhead stability and retraction data were not collected during the 2012 surveys, hence the N/A in the flowhead, and retraction columns for both rounds of 2012 surveys. <sup>b</sup>Rounds 1 and 2 refer to the early and late summer surveys, respectively. <sup>c</sup>WCDD (wetted channel drainage density).

wetted channel networks (WCNs) occupy only 25%, and 24% of the geomorphic channel network for Fox and Elder, respectively (supporting information Figure S2). By the late summer, WCDDs decreased by about 26% to 1.44 and 1.43 km/km<sup>2</sup>, for Fox and Elder, respectively. All major canyons sustain wetted channels, but small, steep, typically boulder-lined first and second-order channels were dry (Figure 9).

Elder south-facing WCDDs were 1.02 km/km<sup>2</sup> in the early 2014 summer, and decreased to 0.33 km/km<sup>2</sup> (over threefold) by late summer, while the WCDD of the north-facing slopes decreased from 1.83 to 1.41 km/km<sup>2</sup> (21.3% decrease), showing some indication of an aspect-induced dry-out affect. However, differences in tree type, thickness of sediment cover in the channel and bedrock critical zone development all likely play a part in this WCDD disparity. Furthermore, the discrepancy in WCDD on north vs south-facing slopes was not as pronounced in the Fox WCN.

Because Fox surveys were completed prior to the Elder surveys, Fox's slightly higher WCDDs (i.e., 0.02 and 0.01 km/km<sup>2</sup> (or 1.3% and 0.7%) greater in Fox than Elder for the early and late summer, respectively) may reflect the slightly higher runoff at the time of survey in Fox. The difference is so small, however, that we conclude that the two watersheds, differing by a factor of six in drainage area, maintain essentially identical WCDDs throughout the summer flow decline.

During many years of research at Angelo, we have only observed overland flow outside of the channel networks (excluding dirt roads and exposed bedrock) once (January 2017). Therefore, using the geomorphic channel drainage density data reported above (section 4.1), and assuming the wetted channel flowhead would not extend beyond the geomorphic channel head, the maximum winter WCDD is 7.9 km/km<sup>2</sup>, yielding a maximum WCDD decline of 81.9% between a possible, but exceptionally rare, peak storm event that completely activates the channel network and the late summer low flows.

Summer 2012 surveys were not as comprehensive, and were therefore more prone to error (see Methods section), but these surveys show the same result of similar WCDDs among the two channel networks. Early summer 2012 WCDDs were 2.09 and 2.01 km/km<sup>2</sup> for Fox and Elder, respectively. By the late summer of 2012, WCDDs had decreased to 1.52 and 1.60 km/km<sup>2</sup> for Fox and Elder, respectively (see Lovill, 2016 for 2012 WCN maps). Despite the much greater annual rainfall in 2012 (1,630 mm) than in 2014 (1,027 mm), the wetted channel densities were only slightly smaller in 2014.

Figure 7 shows that flowhead locations in the Coastal Belt rock (Angelo) are on slopes greater than 10%, but, for a given slope, the contributing drainage area varied by 5 orders of magnitude. Most flowheads drain areas greater than 100 m<sup>2</sup> and some only develop upon draining areas greater than 100,000 m<sup>2</sup>.

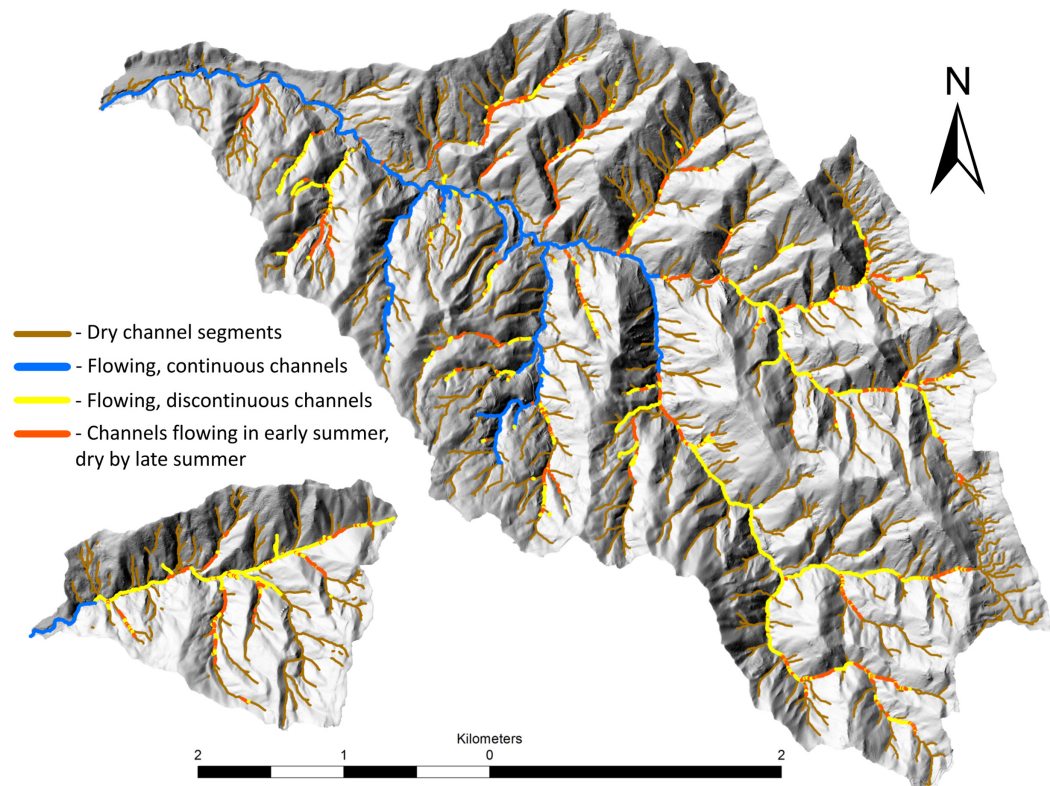


**Figure 9.** (top-right) Elder and (bottom-left) Fox Creek summer 2014 wetted channel maps underlain by shaded relief. The figure shows channel segments that were dry in both the early and late summer (brown), the continuous network (dark blue), the reaches that were dry in the late summer, but wet in the early summer (red), the wetted channel that is not continuously connected to the outflow channel system (yellow). Note that the Fox watershed borders the northwest of the Elder watershed (see Figure 3), but in this figure, it is located southwest of Elder to use space more effectively in the plot.

Unlike the geomorphic channel head (Dietrich & Dunne, 1993), there is neither a simple threshold drainage area, nor slope-drainage area relationship defining where flowheads begin.

#### 4.2.2. Flowhead Stability over Summer Months

Figure 10 shows the late summer wetted channel network (WCN) and location of each flowhead (categorized by type) in Elder Creek. The flowheads were first mapped at the beginning of the summer and part of the categorization of the flowhead is based on whether it became dry or was still flowing in late summer. The flowheads in nontopographically convergent zones typically exist near the base of steep slopes alongside valley bottoms, as compared to the flowheads in convergent areas that occur in upper tributary channels. Flowheads that begin in nontopographically convergent regions correspond to the tips of the geomorphic channel networks: downslope of these flowheads, small channeled valleys extend and join the channel network. Flowheads in the convergent areas were mostly downslope of channel heads and in line with and along the channel network. Surprisingly, 64.1% of all Elder flowheads were at sites with no obvious topographic depression (convergent zone) upslope.

In 2014, in Elder and Fox combined, only 3.9% (3.6% in Elder, and 6.1% in Fox) of the 228 flowheads retracted downslope over the summer months (the red circles in Figure 10). 16.2% (17.4% in Elder, 9.1% in Fox) ceased flowing over the summer months (brown). This leaves 79.8% (79.0% in Elder and 84.8% in Fox) of these flowheads continuing to initiate flow from the exact same location. Furthermore, the retraction of the flowheads in Fox (2 sites) and in Elder (7 sites) accounted for only 2.4% and 1.0% of the total decrease in flow length within the Fox and Elder watersheds, respectively. The discharge out of Elder (and likely Fox) declined by a factor of 6 (0.42–0.07 mm/d) during the summer of 2014. The flowhead stationarity (or lack of flowhead movement downslope) in Fox and Elder throughout the summer of 2014, despite the large

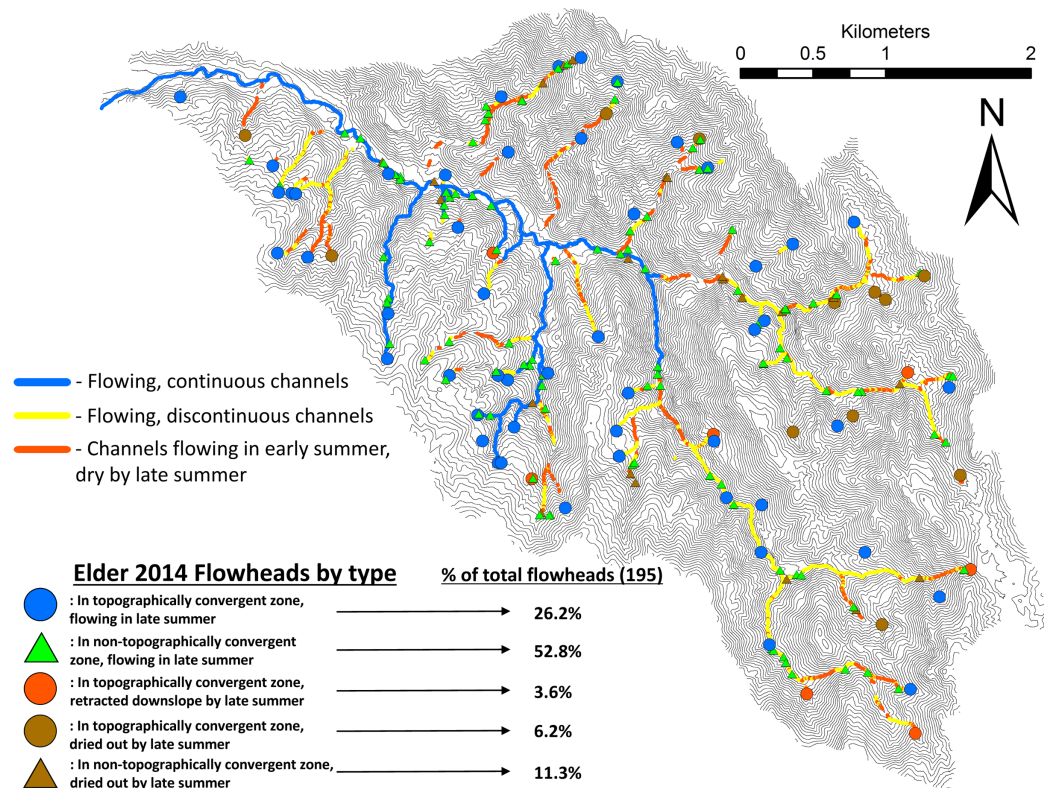


**Figure 10.** Elder Creek flowheads and late summer wetted channels, symbolized by type, underlain by 10 m contours. Wetted channels use the same color coding as Figure 9 (shown in the legend above), with the exception that dry channel segments are represented by blank zones here as opposed to brown lines. Flowheads that originated in convergent areas (hollows) are marked by circles. Flowheads with little or no topographic convergence are marked by triangles. Dynamics are marked by color: fixed and flowing (blue and green), retracted downslope (red), dried up and wetted channel eliminated (brown). The percentage of the total number of Elder flowheads is shown to the right of the flowhead legend. Note that the only retractions were in topographically convergent slopes, hence, there are no red triangles.

decline in discharge, indicates that these springs tapped fixed groundwater sources that declined in drainage rate, but did not become fully depleted.

Additionally, stream water and water emerging from flowheads were nearly isotopically identical in the early and late summer (see supporting information Figure S3). This suggests that water storage within the hillslope is (1) much deeper than the evaporative front and (2) is insensitive to vapor phase diffusion through the unsaturated zone, which confirms our original hypothesis that hillslope water storage occurs deep in the seasonally saturated zone, far below the evaporative front. The only systematic signal observed in the isotope data was a lightening, or isotopic depletion at higher elevations.

#### 4.2.3. Percentage of Elder Creek Discharge from Flowheads

The mapped flowheads define points of visible exfiltrating water (i.e., springs). The distribution of flowheads (in convergent and nonconvergent topographic settings) in both Fox and Elder Creeks indicates that large areas of the watershed likely do not feed visible springs. Figure 10 shows that there are large drainage areas, including entire ridges that drain directly to stream channels but support no surface springs. In those areas, groundwater drainage from hillslopes probably enters streams as either diffuse (and thus difficult to map), exfiltrating flows along the channel walls or bed, or as more concentrated flows that enter the channel below an alluvial infill. These paths were not mappable with the methods employed in this study, but could be identified in future studies by infrared spectroscopy or tracer analysis.

Though the observed flowheads are relatively stationary throughout the summer, the discharge from them clearly declines significantly between early and late summer. To estimate spring discharge, we measured wetted channel width and depth of each springhead and estimated the velocity of flow to be about 2 cm/s in early summer and 1 cm/s in late summer (visual estimation, based on tracing surface floats). This simple

method was employed in order to obtain full channel network surveys within a time period during which discharge would vary little. The velocity likely underestimates values in some of the larger springs. Based on these data, we estimate that the sum of all the individual spring flow rates for early and late summer Elder flowheads was equivalent to 26%, and 23% of the discharge measured at the USGS gaging station in the early and late summer, respectively. The total drainage area (derived from surface topography) of all visible 195 Elder flowheads is equivalent to 27% of Elder's drainage area at the USGS gauging station. However, subsurface fracture flow does not necessarily sense surface topography, so there is a potentially distinct subsurface drainage area. To account for this possibility, we recalculated the drainage area to flowheads, ignoring subtle surface topography and allowing subsurface flow to cross surface topography with less than 3% of the typical vertical relief of a given subcatchment (see supporting information Figure S4 for map of polygons, delineating each Elder flowhead's potential subsurface drainage area). The potential subsurface drainage areas of all Elder flowheads, combined, equated to 34.7% of Elder's drainage area at the USGS gauging station. This value likely represents the highest possible percentage of flowhead drainage area, while 27% represents the low end, suggesting that the true subsurface drainage area is somewhere in between these two values. The similarity of percent drainage area and percent runoff from flowheads, suggest a similar unit area runoff from the rest of the watershed and that this water is arriving via groundwater flow, emerging directly at, or close to the channel.

#### 4.3. Sagehorn Results

##### 4.3.1. Similarities in Adjacent Watershed Wetted Channel Drainage Densities (WCDDs)

During the early summer of 2015, in the Central Belt mélange at Sagehorn, Dry and Hank watersheds (3.54 and 5.59 km<sup>2</sup>, respectively) had WCDDs of 0.86 and 1.22 km/km<sup>2</sup> (Figure 11), respectively, or about half the WCDD at a comparable time in the Coastal Belt Fox and Elder Creeks. By the end of the summer, in both Hank and Dry, wetted channel segments were reduced to either short reaches below springs or isolated pools (Figure 12). As a result, the WCDDs were only 0.15 and 0.12 km/km<sup>2</sup>, in Dry and Hank, respectively. Hence, between the early and late summer surveys, WCDD in Sagehorn decreased by 87.1% (82.5% in Dry and 90.1% in Hank). Figure 12 also shows (in mustard orange) outcrops of sandstone blocks in the mélange. Most springs occurred at the downslope boundary of a sandstone block. Not all blocks, however, emitted springs. Downslope of the late summer flowheads, the wetted channel typically terminated within 5–50 m.

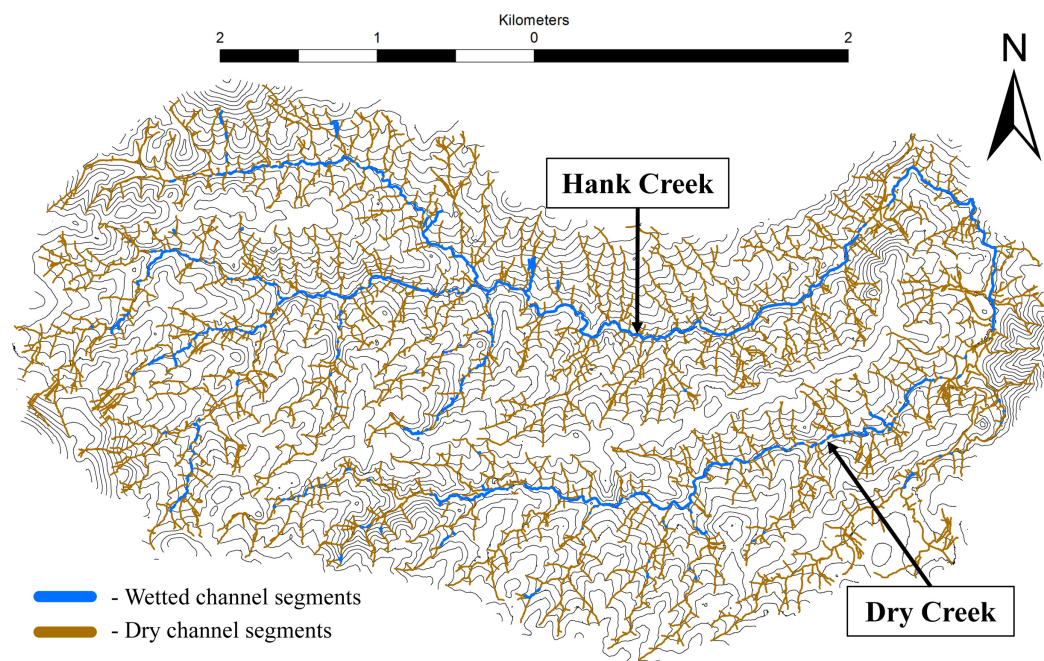


**Figure 11.** (top) Hank and (bottom) Dry early summer wetted channel map, underlain by 10 m contours. Blue lines denote channel segments wetted during the early summer surveys, and brown lines represent dry channels during the early summer 2015 surveys.

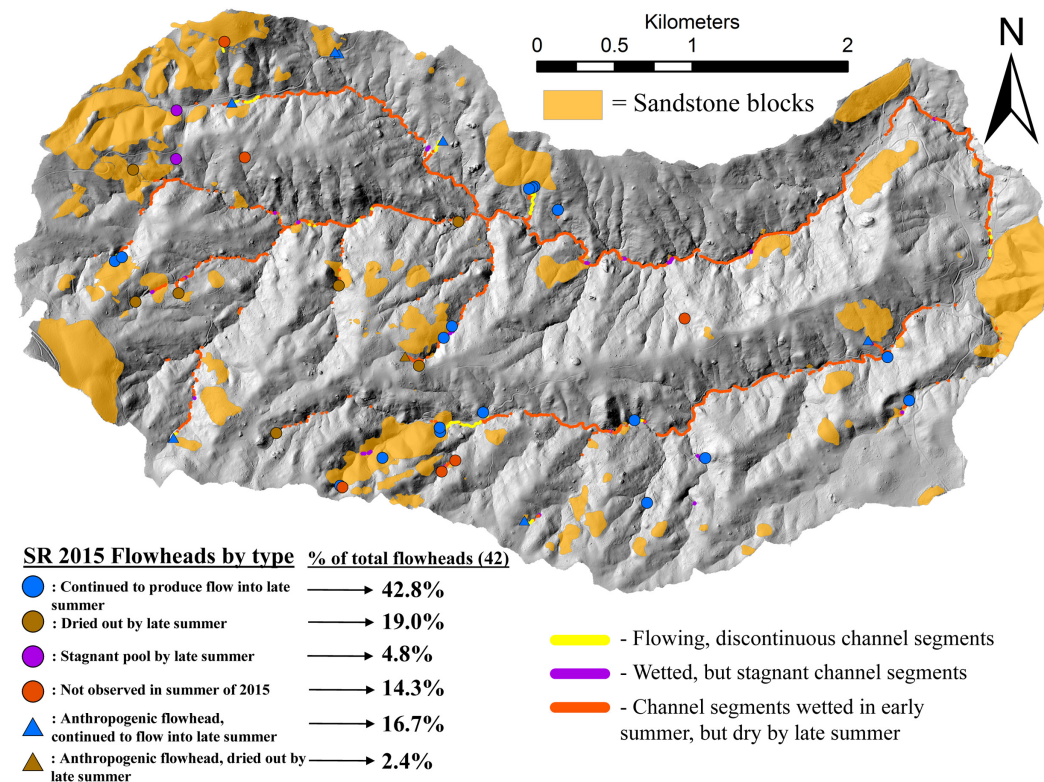


**Figure 12.** Flowheads, and late summer Wetted Channel Network (WCN) for (top) Hank and (bottom) Dry (bottom) Creek watersheds. Sandstone blocks mapped in the field are shown as orange polygons. This figure uses similar wetted channel symbology as Figure 10 (shown in the legend above), however, there is no symbol represented for the continuous channel network because neither Hank, nor Dry have continuous reaches of flow that connect to downstream to Dutch Henry Creek even in early summer. Red channels represent the early summer wetted channels, yellow illustrates late summer wetted channels, and purple delineates stretches of stagnant water. Categories of flowheads in the Sagehorn watersheds are differentiated by whether they continued flowing, dried out, became stagnant, were not observed (represented by blue, brown, purple and red circles, respectively), or whether were anthropogenically forced (i.e., flowheads with piped flow from a storage tank are represented by triangles, see legend above-left). The percentage of the total number of Sagehorn flowheads is shown to the right of the flowhead legend.

During the peak period of winter storms, we observed extensive saturation overland flow that caused the entire channel network to be wet, with flow even extending beyond geomorphic channel heads, up into unchannelled valleys. Hence, using the drainage density value of the entire geomorphic channel network (see section 4.1), during the winter, the Dry and Hank WCDDs were likely greater than  $16.91 \text{ km/km}^2$ .

#### 4.3.2. Flowhead Stability over Summer Months

In the early summer of 2015 in Dry and Hank Creeks, only 37 flowheads were mapped. In early summer of 2016, five additional flowheads were found (suggested by vegetation clustering), which we assume were also present in 2015, bringing the total early summer flowheads to 42. Of these 42 flowheads, 39 were springs emerging from, or downslope of sandstone blocks in the mélange (Figure 12). The early summer survey was completed well after the last significant winter rainfall (30 days). We can conclude that the wetted channels at this time were sustained by drainage from the sandstone blocks. None of the 42 flowheads retracted downslope over the summer months, making all Sagehorn flowheads springs. 38% of the 42 flowheads (29% in Dry and 44% in Hank) ceased flowing by the late summer, leaving 62% (71% in Dry and 56% in Hank) of these flowheads continuing to flow from the same location over the summer months, despite the 87% decrease in WCDD. Because 38% of these flowheads cease to flow by the late summer, the Central Belt hydrologic system is much less stable than the surveyed Coastal Belt watersheds, in which only 20% of flowheads retracted downslope or ceased to flow over the summer months. But, as is the case in Fox and Elder in the Coastal Belt, these data suggest that base flow in the Hank and Dry watersheds of the Central Belt is directly controlled by springs, draining individual storage units.

## 5. Discussion

### 5.1. Lithology, Critical Zone Structure, the Geomorphic Channel Network, and the Wetted Channel Network

The depth and hydraulic properties of the critical zone can exert a primary control on the spatial and temporal extent of wetted channels during summer base flow. Intensive field measurements at our two sites show that the Tóth regional and intermediate flow scales (Figure 1) do not apply, and that there is not a significant connected aquifer that underlies either landscape. Instead, Figure 13 shows two end-member examples, illustrative of conditions we observed: a thick critical zone that can store winter rain as groundwater and deliver sustained base flow, and a shallow critical zone of limited storage, in which channels in the summer become dry. Model 1 illustrates the thick critical zone observed in Rivendell (Salve et al., 2012), likely ubiquitous throughout the Coastal Belt, and Model 2 exemplifies the thin critical zone, observed at Sagehorn and likely common elsewhere in the Central Belt mélange. The low hydraulic conductivity of underlying fresh shale and mélange matrix forces the hydrologic dynamics in both lithologies to be constrained to the weathered zone of hillslopes. The Coastal Belt's lack of temporal variability in WCDD points to a fixed fracture system, draining groundwater in the critical zone. This groundwater receives sufficient recharge during winter months to sustain the WCN throughout the summer. Most of the flow in the summer reaches streams without a spring surface expression. These flows also likely travel via fracture networks which likely dominate the conductive porosity at depth (Salve et al., 2012).

Compared to the WCDDs at Angelo in the Coastal Belt, Sagehorn, in the Central belt mélange, has lower early summer and dramatically lower late summer densities. The thin critical zone there provides little storage. Most springs in the mélange originated in the large sandstone blocks, where storage is more like that

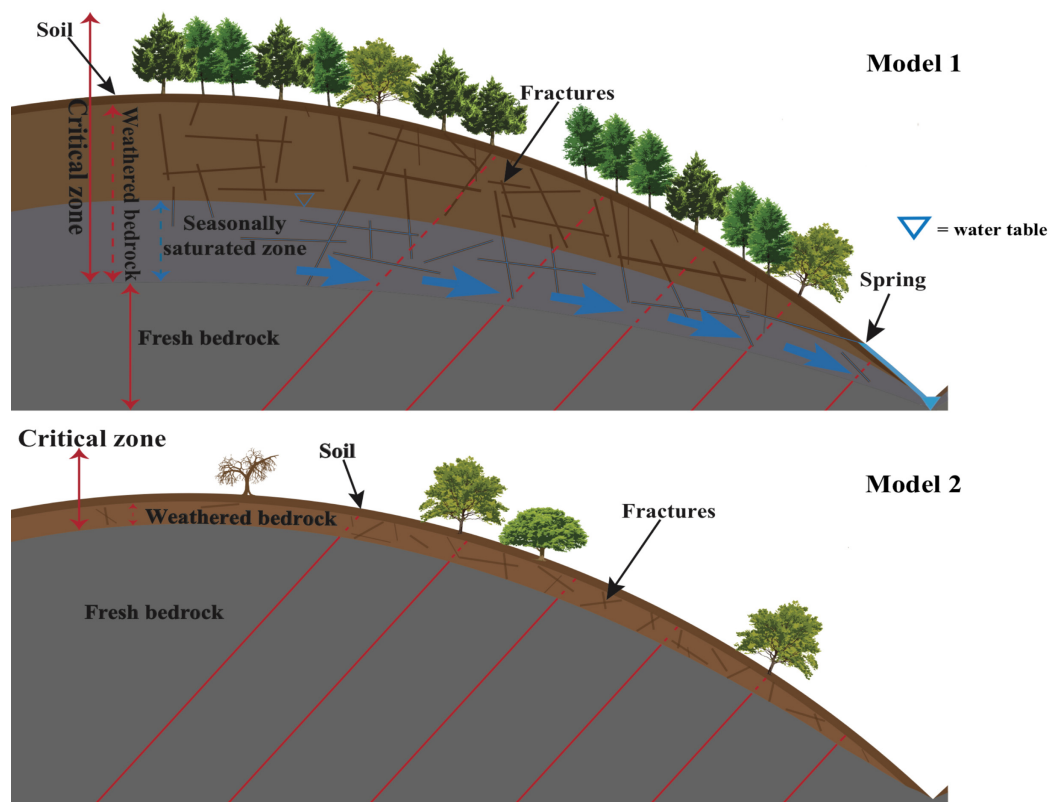


**Figure 13.** Conceptual models of potential hillslope water storage and sustained base flow related to thickness of weathered bedrock zone during summer months. The red lines represent bedrock structure (such as bedding). In Model 1, groundwater stored in the weathered bedrock during the wet season flows downslope, emerges as springs, and enters the channel (represented by the sky-blue triangle at the base of the hillslope). The depth and structure of the weathered bedrock zone determines the volume of potential groundwater storage. In Model 2, the thin critical zone prevents significant groundwater storage and sustained base flow, consequently the channel is dry.



**Figure 14.** Boulder fill in the Elder Creek main stem at 4.5 km from the mouth. Local slope is 50% even though the upslope drainage area is  $3.0 \text{ km}^2$ . Individual in the photograph is 190 cm tall.

that there is a similarity in process that suggests that the general principles, controlling the extent of wetted channels at our study sites, may be broadly applicable to the larger Eel River watershed, which is dominated by the Coastal and Central Belts (Langenheim et al., 2013). The observation that in the same climatic setting, the landscape with the greater geomorphic channel density has the far lower summer wetted channel density, suggests caution in relying on topographic data alone to infer potential wetted channel extent.

### 5.2. Geomorphic History and the Influence of Disconnections and Channel Fill Within the Geomorphic Channel Network on the WCN

Seepage into thick sediment deposits can completely drain surface flow and thereby prevent continuous wetted channel development (e.g., Godsey & Kirchner, 2014; Queener & Stubblefield, 2016; Whiting & Godsey, 2016). In the lower reaches of Elder (downstream of the first major knickpoint), the channel is mostly covered by thin alluvium with a depth of only a few coarse grain diameters. Upstream, the main stem and most of the tributaries and the upper portion of Elder Creek are mantled with a much thicker layer of coarse sediment (Figure 14) generated in the late Pleistocene and Holocene. Figure 15 records the occurrence of this thick fill and of the large debris flow fans that have built into the main stem from the tributaries. It is striking that the continuous wetted channel approximately corresponds to the main stem reach where upslope knickpoint propagation has removed the coarse thick fill (still quite visible in the strath terrace alluvial caps downstream of the knickpoint). It is this wetted channel that also sustains steelhead populations (Kelson et al., 2016). Hence, the wetted channel extent and its ecological consequences are strongly influenced by the geomorphic history of channel incision and sediment delivery.

### 5.3. Fracture Flow and Wetted Channel Dynamics

Several recent field studies infer that fracture flow (in the critical zone) influences the location and persistence of springs and the magnitude of base flow. Payn et al. (2012) explored controls on base flow during seasonal recession in a  $23 \text{ km}^2$  watershed in Montana, where a canyon system had cut through a sandstone cap into underlying granite-gneiss, and proposed that as flows declined, their relationship to drainage area

found in the Coastal Belt. Even in the early summer surveys, a substantial portion of the water that was present in the main stem of Hank and Dry was stagnant, or nearly stagnant. The differences in WCDD between Hank and Dry reverse between early and late summer: Hank maintains a greater WCDD than Dry in early summer, but Dry exceeds Hank's very low WCDD in late summer. This variability may be tied to the changing influence of the springs, discharging from heterogeneous sandstone blocks, the primary source of base flow in these channels. While the thin critical zone over the argillaceous-matrix mélange and watersheds within mélange are likely to have limited wetted channels, the proportion of sandstone blocks will vary widely among watersheds, and so might, then, the persistence of summer base flow and the WCDD.

We hypothesize that sandstone blocks embedded within mélange matrix that extend well below the 3 m level (the depth to fresh, non-conductive bedrock, Hahm et al., 2016) remain saturated with stagnant water. These blocks are weathered and fractured and thus can store and release water. Rain and snowmelt will enter the sandstone fracture system, encounter the impermeable mélange boundary and build a local dynamic water table within the block. Emergent sandstone blocks, with significant relief above adjacent mélange matrix, can become, in essence, islands of drainable, seasonally replenished water, sitting in a sea of perennially saturated, nondraining mélange.

The general similarity of WCN and WCDD dynamics between adjacent watersheds in both the Central and the Coastal Belt suggests a similarity of critical zone development across this landscape, and reflects a similarity of geomorphic channel structure. This finding is relevant for regional watershed management and modeling because it implies

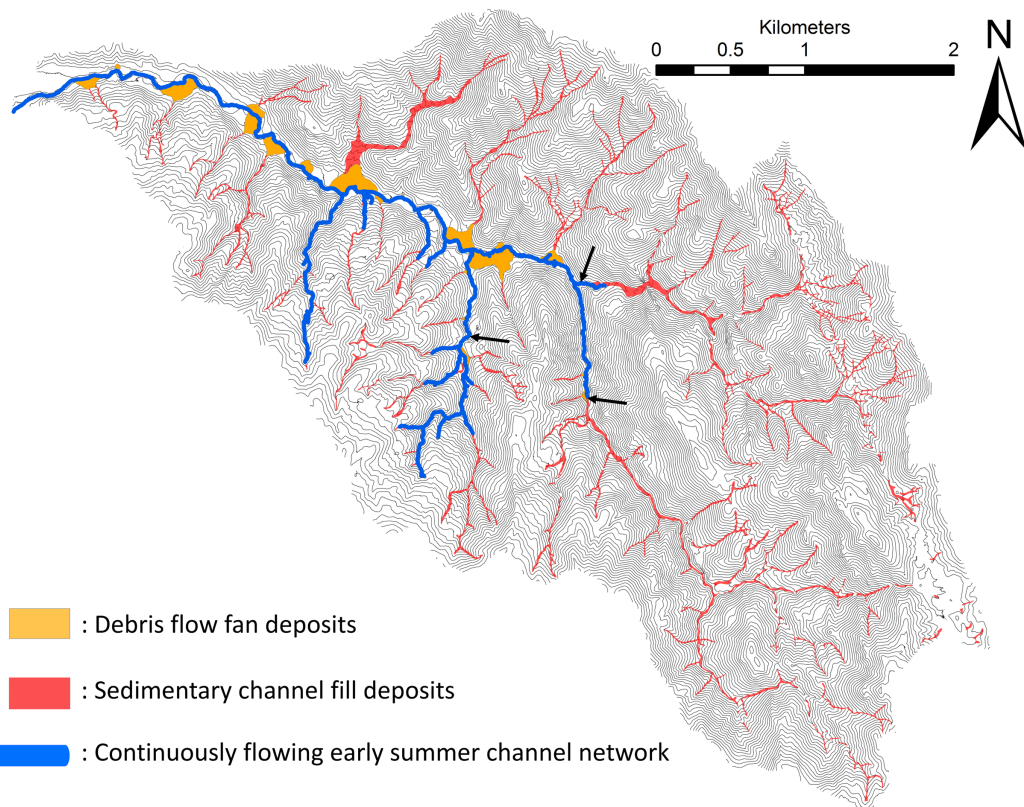


**Figure 15.** Elder Creek geomorphic history related to channel fill, and debris flow fans. Channels with thick deposits of sediment (red) and fans (orange) formed by debris flow deposition. Debris flow fans are found at the mouths of many smaller tributaries, but are too small to be shown clearly on this map. Blue lines represent the late summer continuous flow network. Black arrows represent the location of the major knickpoints along the main channels. Thin, black lines represent 10 m contours..

diminished, and deeper flows, directed by fractures, dominated base flow. Multiple studies have observed fracture flow sustaining perennial springs in basins underlain by granite (e.g., Asano et al., 2002; Onda et al., 2004). Whiting and Godsey (2016) surveyed wetted channels and flowheads in Central Idaho in a watershed mostly underlain by granodiorite. With decreasing summer runoff, most flowheads remained stationary and the extent of wetted channels exhibited relatively small reductions (decreases occurred where the flow seeped into the sediment fill). They inferred that this persistence occurred because of sustained groundwater flow, directed to the surface via bedrock fractures. Shaw (2016) tracked wetted channel changes during recession in a small watershed underlain by shales and siltstone in New York. He found that the location of perennial flowing “groundwater seeps” controlled the spatial extent of the WCN. Disconnections downslope of flowheads (due to alluvial fill infiltration) accounted for most of the decrease in wetted channel length (similar to what we observed in the surveyed WCNs). Shaw speculated that bedrock fractures could direct and localize flow to form the observed seeps in some areas.

In contrast to these studies, Godsey and Kirchner (2014) report flowhead instability and substantial changes in extent of wetted channel with discharge. We have visited one of their study sites, just 31 km away from Angelo and similarly underlain by the Coastal Belt (Figure 2). Our observations indicate that the Caspar Creek watershed, although underlain by similar lithology, has a far greater relative percentage of highly weathered sandstone, and consequently less argillite than Angelo. Nonetheless, Brown (1995) documented a dynamic groundwater table in an upslope thickening saprolite on a steep hillslope in Caspar, similar in pattern to the Rivendell hillslope at Angelo. Some of the difference between the Angelo channel networks and Caspar Creek may be due to the 35% more annual precipitation at Angelo than Caspar (precipitation data from Godsey & Kirchner, 2014), but this difference is small compared to the large difference in WCDD.

Unlike Angelo, the old growth forest in Caspar was clear-cut for timber in the late 1800s, then burned (Tilley & Rice, 1977), before multiple flash-dams were established (Cafferata & Spittler, 1998). Further disturbance occurred throughout the late 1960s and early 1970s when roads were constructed and most of the secondary forest was again harvested, leading to major fluctuations in sediment yield (Adams et al., 2004), primarily due to a substantial number of landslides (Cafferata & Spittler, 1998). The legacy effect of the relatively thick depth of sediment fill throughout Caspar's WCN has clearly had a profound influence on Caspar's WCDD values. Godsey and Kirchner (2014) report WCDD values ranging from 0.50 to 0.99 km/km<sup>2</sup> in Caspar Creek (8.48 km<sup>2</sup>) (while we observed values ranging from 1.43 to 1.95 km/km<sup>2</sup> in Angelo). Together, these observations suggest that the more dynamic WCDD in Caspar than at the Angelo probably arises from legacy effects of sedimentation of the channel network.

#### 5.4. Critical Zone Drainage and Sustained Wetted Channels during Drought

Watersheds concentrate runoff and consequently relatively small flows can sustain wetted channels, if channel sediment fills are not too thick. The extreme dry year of 2014 illustrates that large variations in precipitation between years can still replenish the critical zone, enabling drainage that sustains a thriving salmon population. As a case in point, the winter rainfall leading to our 2014 wetted channel summer surveys was about 1/2 of average (1,027 mm relative to the 1985–2016 Angelo average of 1,853 mm). In the previous 2012 survey the rainfall was 1,630 mm. These differences might be expected to result in a much lower WCDD in 2014. This was not the case (see Table 1). Between the two summer surveys in 2014, the total runoff was just 15.0 mm, or 0.18 mm/d. In 2012 the total runoff for a shorter period was 12.2 mm (0.20 mm/d).

Observations at our Rivendell study site show that the groundwater levels dropped between 0.7 and 2.7 m at various positions along the hillslope profile during the 2012 and 2014 summer surveys. This is consistent with low porosity in the weathered rock near the base of the critical zone (i.e., relatively large ground water level drop to sustain relatively small summer runoff). Although limited in storage, low saturated conductivity results in slow drainage, and thus, sustained streamflow throughout even very dry years. Hence, the critical zone structure, its thickness, porosity, and saturated conductivity are expressed in the extent and persistence of the wetted channel network.

#### 5.5. Sandstone Blocks, Water Sources, and Land Management in the Central Belt Mélange

Agricultural use across the Central Belt mélange in the Eel River watershed consists primarily of cattle and cannabis production. The most impacted resource, related to both these products, is water. In both cases, landowners have learned to exploit the springs from the sandstone blocks, although the severe limitation that these blocks represent (i.e., they are the only source of readily extractible groundwater) is not widely appreciated. Furthermore, it has not been previously recognized that the extent of wetted channels in the summer, and the ecosystem they support, depends entirely on spring flow from the sandstone blocks.

Specific tree species inhabit sandstone blocks (Douglas fir (*Pseudotsuga menziesii*), madrone (*Arbutus menziesii*), tanoak (*Notholithocarpus densiflorus*), California bay laurel (*Umbellularia californica*), and California black oak (*Quercus kelloggii*)) (Hahm et al., 2017), and these tree species have specific pigmentation, such that they are identifiable via aerial imagery. In the mélange, these tree species grow primarily on sandstone blocks, while Oregon White Oaks (*Quercus garryana*) and grassland inhabit the mélange matrix (Hahm et al., 2017). Therefore, noting the position of these tree types should help identify the location, and size of sandstone blocks, and therefore potential springs, which should be informative for management practices to understand where water might be located.

The growth of cannabis is becoming an increasingly important issue in Northern California, and especially Mendocino County, both economically and environmentally (Bauer et al., 2015; Carah et al., 2015, Mallery, 2011; Mills, 2012). Given the current profitability of cannabis production, Butsic and Brenner (2016) expect that cannabis agriculture will expand into other sites with suitable growing conditions throughout Northern California. If multiple flowheads that would have ordinarily supplied flow for a tributary are instead diverted for irrigation, entire tributaries could go dry during summer months. The integrated effect of such small-scale diversions could result in larger rivers that host salmonids and other native species at heightened risk of drying and/or overheating. In light of this growing threat to Northern California water resources, our findings highlight the potential sensitivity of downstream flows to extraction at flow sources and underscore the need for their protection and management.

### 5.6. Future Wetted Channel Surveys

Mapping the full extent of wetted channels in a watershed currently requires a major investment in time and physical effort. More maps are needed to develop general understanding of controls and to stimulate modeling efforts. Based on our experience and our review of other studies on wetted channel networks (WCNs), we suggest that it is important to document discharge from flowheads, in addition to the four other important attributes of headwater WCNs described in the introduction.

Wetted channel surveys need to be quantitatively linked to critical zone structure and channel geomorphic history. Detailed observations of critical zone structure help to reveal controls on flux rates and locations of flowheads. Such intrahillslope understanding complements geomorphic studies that can explain the spatial pattern of channel fills and their effect on wetted channel continuity. Our analysis after data collection indicates that measuring discharge from flowheads is very important in understanding what proportion of total discharge is entering the system via flowheads, versus groundwater, throughout the watershed.

High-resolution topographic data (e.g., 1 m contour quality data) are essential to accurately note wetted versus dry stream lengths, and the exact positions of flowheads. Godsey and Kirchner (2014) and Whiting and Godsey (2016) used GPS data to track flowhead positions, and wetted channel segments. This is a practical, if less precise method, where high-resolution topographic data are lacking. However, steep canyon walls and dense vegetation can work to decrease the accuracy of most GPS systems.

## 6. Conclusions

In the argillite dominated Coastal Belt in Northern California, a thick conductive critical zone has developed in which groundwater accumulates in winter and slowly drains in summer to adjacent channels. This summer groundwater drainage likely travels along fractures to surface point sources (flowheads), and water either enters the channel network through flowheads, or directly to channels via groundwater seepage. This sustained slow flow supports the wetted channel network (WCN) throughout the summer, producing relatively high wetted channel drainage densities (WCDDs) in Fox and Elder networks. In contrast, in the Central Belt mélange, the thin critical zone seasonally saturates, sheds most water, and rapidly drains, providing limited storage. By the late summer, the only flowing water in the drainage networks emerges from point sources, sustained by storage reservoirs within sandstone blocks. These sandstone blocks, embedded within the mélange, represent a special case of critical zone evolution: two different lithologies with contrasting material properties, leading to distinct critical zone depths and water storage potentials in one watershed. The differences in critical zone properties cause the Coastal Belt site to be a “water storing” landscape, while the Central Belt site is a “water shedding” landscape.

Geomorphic history, related to channel fill, affects the extent and continuity of the wetted channels. In the Coastal Belt, coarse, thick deposits of sediment blanket most of the channel network of Fox and Elder Creek. This sediment may have accumulated during the late Pleistocene, when climate conditions likely favored landslide activity. Holocene incision into this sediment and into the underlying bedrock has propagated upstream. The extent of the continuous summer WCN is defined by the termination points of incision upstream. Residual thick, conductive sediment upslope of incision termination points in the channels leads to stream flow infiltrating, rather than persisting on the surface. This hyporheic flow is consequently a major cause of summer flow discontinuity.

Underlying lithology, critical zone evolution, and geomorphic channel network development exert a primary control on the extent and persistence of wetted channels for a given climatic setting. The depth of channel fill, and other factors, associated with geomorphic history of the landscape, can have a strong local effect on the amount of surface flow expressed in the channel. This suggests that future studies of wetted channel networks should be done within a strong geomorphic and critical zone context. Such studies will guide the development of quantitative models of wetted channels extent, dynamics and responses to droughts, vegetation change, and base flow extraction by humans.

## References

- Acuña, V., Hunter, M., & Ruhi, A. (2017). Managing temporary streams and rivers as unique rather than second-class ecosystems. *Biological Conservation*, 211, 12–19.

## Acknowledgments

The research was supported by the National Science Foundation EAR-1331940 grant for the Eel River Critical Zone Observatory with additional support from the Mildred E. Mathias Graduate Student Research Grant. The National Center for Airborne Laser Mapping provided lidar coverage of both field sites. Data supporting the results and conclusions are available in Lovill (2016) and at <http://criticalzone.org/eel/publications/>. Tom Ogasawara, Jennifer Rose, and Claire Wilkin assisted in the extensive fieldwork. Collin Bode helped integrate field data into ARC GIS. Daniella Rempe, Jasper Oshun, Mary Power, Todd Dawson, and Inez Fung provided useful comments and edits on an earlier draft. Gordon Grant, two anonymous reviewers, and the Water Resources Editor (Ilja van Meerveld) provided valuable comments and recommendations. A final thanks to Marilyn and Jerry Russell and the Holleman family for their kindness and openness in allowing our group access to their land for field research and for providing many useful observations.

- Adams, M. B., Loughry, L. H., & Plaugher, L. L. (2004). *Experimental forests and ranges of the USDA Forest Service* (Gen. Tech. Rep. NE-321). Newtown Square, PA: U.S. Department of Agriculture, Forest Service, Northeastern Research Station.
- Anderson, S. P., Dietrich, W. E., & Brimhall, G. H. (2002). Weathering profiles, mass-balance analysis, and rates of solute loss: Linkages between weathering and erosion in a small, steep catchment. *Geological Society of America Bulletin*, 114(9), 1143–1158.
- Arroita, M., Flores, L., Larrañaga, A., Martínez, A., Martínez-Santos, M., Pereda, O., et al. (2017). Water abstraction impacts stream ecosystem functioning via wetted-channel contraction. *Freshwater Biology*, 62(2), 243–257.
- Asano, Y., Uchida, T., & Ohte, N. (2002). Residence times and flow paths of water in steep unchannelled catchments, Tanakami, Japan. *Journal of Hydrology*, 261(1), 173–192.
- Asarian, J. E., & Walker, J. D. (2016). Long-term trends in streamflow and precipitation in Northwest California and Southwest Oregon, 1953–2012. *Journal of the American Water Resources Association*, 52(1), 241–261.
- Bauer, S., Olson, J., Cockrill, A., van Hattem, M., Miller, L., Tauzer, M., et al. (2015). Impacts of surface water diversions for marijuana cultivation on aquatic habitat in four northwestern California watersheds. *PLoS One*, 10(3), e0120016.
- Bencala, K. E., Gooseff, M. N., & Kimball, B. A. (2011). Rethinking hyporheic flow and transient storage to advance understanding of stream-catchment connections. *Water Resources Research*, 47, W00H03. <https://doi.org/10.1029/2010WR010066>
- Bennett, G. L., Miller, S. R., Roering, J. J., & Schmidt, D. A. (2016). Landslides, threshold slopes, and the survival of relict terrain in the wake of the Mendocino Triple Junction. *Geology*, 44(5), 363–366.
- Biswal, B., & Nagesh Kumar, D. (2013). A general geomorphological recession flow model for river basins. *Water Resources Research*, 49, 4900–4906. <https://doi.org/10.1002/wrcr.20379>
- Blake, M. C., Jayko, A. S., McLaughlin, R. J., & Underwood, M. B. (1988). Metamorphic and tectonic evolution of the Franciscan Complex, Northern California. In W. G. Ernst (Ed.), *Metamorphism and crustal evolution of the western United States, Rubey Colloquium Series* (Vol. VII, pp. 1036–1059). Englewood Cliffs, NJ: Prentice Hall.
- Broda, S., Larocque, M., Paniconi, C., & Haitjema, H. (2012). A low-dimensional hillslope-based catchment model for layered groundwater flow. *Hydrological Processes*, 26(18), 2814–2826.
- Broda, S., Larocque, M., & Paniconi, C. (2014). Simulation of distributed base flow contributions to streamflow using a hillslope-based catchment model coupled to a regional-scale groundwater model. *Journal of Hydrologic Engineering*, 19(5), 907–917.
- Brown, D. L. (1995). *An analysis of transient flow in upland watersheds: Interactions between structure and process* (PhD dissertation, 225 p.). Berkeley, CA: University of California.
- Butsic, V., & Brenner, J. C. (2016). Cannabis (*Cannabis sativa* or *C. indica*) agriculture and the environment: A systematic, spatially-explicit survey and potential impacts. *Environmental Research Letters*, 11(4), 044023.
- Cafferata, P. H., & Spittler, T. E. (1998). *Logging impacts of the 1970's vs. the 1990's in the Caspar Creek watershed* (Gen. Tech. Rep. PSW-GTR-168, pp. 103–115), Albany, CA: PSW Research Station, USDA Forest Service.
- Carah, J. K., Howard, J. K., Thompson, S. E., Gianotti, A. G. S., Bauer, S. D., Carlson, S. M., et al. (2015). High time for conservation: Adding the environment to the debate on marijuana liberalization. *BioScience*, 65(8), 822–829.
- Clark, M. P., Rupp, D. E., Woods, R. A., Tromp-van Meerveld, H. J., Peters, N. E., & Freer, J. E. (2009). Consistency between hydrological models and field observations: Linking processes at the hillslope scale to hydrological responses at the watershed scale. *Hydrological Processes*, 23(2), 311–319.
- Cloos, M. (1982). Flow melanges: Numerical modeling and geologic constraints on their origin in the Franciscan subduction complex, California. *Geological Society of America Bulletin*, 93(4), 330–345.
- Danehy, R. J., Bilby, R. E., Owen, S., Duke, S. D., & Farrand, A. (2017). Interactions of base flow habitat constraints: Macroinvertebrate drift, stream temperature, and physical habitat for anadromous salmon in the Calapooia River, Oregon. *Aquatic Conservation*, 27, 653–662.
- Dietrich, W. E., & Dunne, T. (1993). The channel head, in K. Beven & M. J. Kirkby (Eds.), *Channel Network Hydrology* (pp. 175–219). Hoboken, NJ: J. Wiley & Sons.
- Dralle, D. N., Karst, N. J., & Thompson, S. E. (2016). Dry season streamflow persistence in seasonal climates. *Water Resources Research*, 52, 90–107. <https://doi.org/10.1002/2015WR017752>
- Dralle, D. N., Hahm, W. J., Rempe, D. M., Karst, N. J., Thompson, S. E., & Dietrich, W. E. (2018). Quantification of the seasonal hillslope water storage that does not drive streamflow. *Hydrological Processes*. <https://doi.org/10.1002/hyp.11627>
- Druhan, J. L., Fernandez, N., Wang, J., Dietrich, W. E., & Rempe, D. (2017). Seasonal shifts in the solute ion ratios of vadose zone rock moisture from the EEL River Critical Zone Observatory. *Acta Geochimica*, 36(3), 385–388.
- Dumitru, T. A., Wakabayashi, J., Wright, J. E., & Wooden, J. L. (2010). Early Cretaceous transition from nonaccretionary behavior to strongly accretionary behavior within the Franciscan subduction complex. *Tectonics*, 29, TC5001. <https://doi.org/10.1029/2009TC002542>
- Ernst, W. G. (1970). Tectonic contact between the Franciscan mélange and the Great Valley sequence: Crustal expression of a late Mesozoic Benioff zone. *Journal of Geophysical Research*, 75(5), 886–901.
- Ernst, W. G., & McLaughlin, R. J. (2012). Mineral parageneses, regional architecture, and tectonic evolution of Franciscan metagraywackes, Cape Mendocino-Garberville-Covelo 30° × 60' quadrangles, northwest California. *Tectonics*, 31, TC1001. <https://doi.org/10.1029/2011TC002987>
- Finnegan, N. J., & Dietrich, W. E. (2011). Episodic bedrock strath terrace formation due to meander migration and cutoff. *Geology*, 39(2), 143–146.
- Frisbee, M. D., Tyson, E. H., Stewart-Maddox, N. S., Tsinnajinnie, L. M., Wilson, J. L., Granger, D. E., et al. (2016). Is there a geomorphic expression of interbasin groundwater flow in watersheds? Interactions between interbasin groundwater flow, springs, streams, and geomorphology. *Geophysical Research Letters*, 43, 1158–1165. <https://doi.org/10.1002/2015GL067082>
- Fuller, T. K., Perg, L. A., Willenbring, J. K., & Lepper, K. (2009). Field evidence for climate-driven changes in sediment supply leading to strath terrace formation. *Geology*, 37(5), 467–470.
- Gleeson, T., & Manning, A. H. (2008). Regional groundwater flow in mountainous terrain: Three-dimensional simulations of topographic and hydrogeologic controls. *Water Resources Research*, 44, W10403. <https://doi.org/10.1029/2008WR006848>
- Godsey, S. E., & Kirchner, J. W. (2014). Dynamic, discontinuous stream networks: Hydrologically driven variations in active drainage density, flowing channels and stream order. *Hydrological Processes*, 28(23), 5791–5803.
- González-Ferreras, A. M., & Barquín, J. (2017). Mapping the temporary and perennial character of whole river networks. *Water Resources Research*, 53, 6709–6724. <https://doi.org/10.1029/2017WR020390>
- Hamada, Y., O'Connor, B. L., Orr, A. B., & Wuthrich, K. K. (2016). Mapping ephemeral stream networks in desert environments using very-high-spatial-resolution multispectral remote sensing. *Journal of Arid Environments*, 130, 40–48.

- Hahm, W. J., Dietrich, W. E., Dawson, T. E., Lovill, S., & Rempe, D. (2016). *Ecohydrological consequences of critical zone structure in the Franciscan formation, Northern California Coast Ranges*. Abstract EP41F-07 presented at AGU Fall Meeting. San Francisco: American Geophysical Union.
- Hahm, W. J., Dietrich, W. E., & Dawson, T. E. (2018). Controls on the distribution and resilience of *Quercus garryana*: Ecophysiological evidence of oak's water-limitation tolerance. *Ecosphere*, 9(5). <https://doi.org/10.1002/ecs2.2218>
- Hahm, W. J., Dietrich, W. E., Rempe, D. M., Dralle, D. N., Dawson, T. E., Lovill, S., et al. (2017). *The influence of critical zone structure on runoff paths, seasonal water storage, and ecosystem composition (Invited)*. Abstract U13B-37 presented at AGU Fall Meeting. New Orleans, LA: American Geophysical Union.
- Hahm, W. J., Dralle, D. N., Lovill, S. M., Rose, J., Dawson, T., & Dietrich, W. E. (2017). *Exploratory tree survey (2016 - Eel River critical zone observatory - Sagehorn - Central Belt Melange, Franciscan Complex, Northern California Coast Ranges, USA)*, HydroShare. <https://doi.org/10.4211/hs.7881821a5c0e4ae3822b96a59f4bf8b6>.
- Hladz, S., Watkins, S. C., Whitworth, K. L., & Baldwin, D. S. (2011). Flows and hypoxic blackwater events in managed ephemeral river channels. *Journal of Hydrology*, 401(1), 117–125.
- Holbrook, W. S., Riebe, C. S., Elwaseif, M., L Hayes, J., Basler-Reeder, K., Harry, D. L. et al. (2014). Geophysical constraints on deep weathering and water storage potential in the Southern Sierra Critical Zone Observatory. *Earth Surface Processes and Landforms*, 39(3), 366–380.
- Jaeger, K. L., Olden, J. D., & Pelland, N. A. (2014). Climate change poised to threaten hydrologic connectivity and endemic fishes in dryland streams. *Proceedings of the National Academy of Sciences of the United States of America*, 111(38), 13894–13899.
- Johnson, S. G. (1979). *The land-use history of the coast range preserve, Mendocino County, California* (MS thesis). San Francisco, CA: San Francisco State University.
- Kelson, S., Miller, M., & Carlson, S. M. (2016). *The influence of geomorphology and hydrology on O. mykiss life history zonation in streams*. Abstract presented at 2016 Pacific Coast Steelhead Management Meeting Abstracts. Berkeley, CA: University of California.
- Kim, H., Bishop, J. K., Dietrich, W. E., & Fung, I. Y. (2014). Process dominance shift in solute chemistry as revealed by long-term high-frequency water chemistry observations of groundwater flowing through weathered argillite underlying a steep forested hillslope. *Geochimica et Cosmochimica Acta*, 140, 1–19.
- Kim, H., Dietrich, W. E., Thurnhoffer, B. M., Bishop, J. K., & Fung, I. Y. (2017). Controls on solute concentration-discharge relationships revealed by simultaneous hydrochemistry observations of hillslope runoff and stream flow: The importance of critical zone structure. *Water Resources Research*, 53, 1424–1443. <https://doi.org/10.1002/2016WR019722>
- Kirchner, J. W. (2009). Catchments as simple dynamical systems: Catchment characterization, rainfall-runoff modeling, and doing hydrology backward. *Water Resources Research*, 45, W02429. <https://doi.org/10.1029/2008WR006912>
- Lake, P. S. (2003). Ecological effects of perturbation by drought in flowing waters. *Freshwater Biology*, 48(7), 1161–1172.
- Langenheim, V. E., Jachens, R. C., Wentworth, C. M., & McLaughlin, R. J. (2013). Previously unrecognized regional structure of the Coastal Belt of the Franciscan Complex, northern California, revealed by magnetic data. *Geosphere*, 9(6), 1514–1529.
- Larned, S. T., Arscott, D. B., Schmidt, J., & Dietrich, J. C. (2010). A framework for analyzing longitudinal and temporal variation in river flow and developing flow-ecology relationships1. *Journal of the American Water Resources Association*, 46(3), 541–553.
- Lebedeva, M. I., & Brantley, S. L. (2013). Exploring geochemical controls on weathering and erosion of convex hillslopes: Beyond the empirical regolith production function. *Earth Surface Processes and Landforms*, 38(15), 1793–1807.
- Link, P., Simonin, K., Maness, H., Oshun, J., Dawson, T., & Fung, I. (2014). Species differences in the seasonality of evergreen tree transpiration in a Mediterranean climate: Analysis of multiyear, half-hourly sap flow observations. *Water Resources Research*, 50, 1869–1894. <https://doi.org/10.1002/2013WR014023>
- Liu, C., Wang, L., Xin, Z., & Li, Y. (2017). Comparative study of wet channel network extracted from LiDAR data under different climate conditions. *Hydrology Research*, 49(2), nh2017255.
- Lock, J., Kelsey, H., Furlong, K., & Woolace, A. (2006). Late Neogene and Quaternary landscape evolution of the northern California Coast Ranges: Evidence for Mendocino triple junction tectonics. *Geological Society of America Bulletin*, 118(9–10), 1232–1246.
- Lovill, S. M. (2016). Drainage from the critical zone: Lithologic, aspect, and vegetation controls on the persistence and spatial extent of wetted channels during the summer dry season (MS thesis). Berkeley, CA: University of California.
- Mackey, B. H., Scheingross, J. S., Lamb, M. P., & Farley, K. A. (2014). Knickpoint formation, rapid propagation, and landscape response following coastal cliff retreat at the last interglacial sea-level highstand: Kaua'i, Hawai. *Geological Society of America Bulletin*, 126(7–8), 925–942.
- Malard, F., Uehlinger, U., Zah, R., & Tockner, K. (2006). Flood-pulse and riverscape dynamics in a braided glacial river. *Ecology*, 87(3), 704–716.
- Mallery, M. (2011). Marijuana national forest: Encroachment on California public lands for cannabis cultivation. *Berkeley Undergraduate Journal*, 23(2), 1–50.
- McKee, C. J., Stewart, K. M., Sedinger, J. S., Bush, A. P., Darby, N. W., Hughson, D. L., et al. (2015). Spatial distributions and resource selection by mule deer in an arid environment: Responses to provision of water. *Journal of Arid Environments*, 122, 76–84.
- McLaughlin, R. J., Ellen, S. D., Blake, M. C., Jr., Jayko, A. S., Irwin, W. P., Aalto, K. R., et al., (2000). *Geology of the Cape Mendocino, Eureka, Garberville, and Southwestern Part of the Hayfork 30 x 60 minute Quadrangles and adjacent offshore area, Northern California* (Miscellaneous Field Studies Map MF-2336, pp. 1–16). Reston, VA: U.S. Geological Survey.
- McNamara, J. P., Tetzlaff, D., Bishop, K., Soulsby, C., Seyfried, M., Peters, N. E., et al. (2011). Storage as a metric of catchment comparison. *Hydrological Processes*, 25(21), 3364–3371.
- Mills, E. (2012). The carbon footprint of indoor Cannabis production. *Energy Policy*, 46, 58–67.
- Montgomery, D. R., & Buffington, J. M. (1997). Channel-reach morphology in mountain drainage basins. *Geological Society of America Bulletin*, 109(5), 596–611.
- Onda, Y., Tsujimura, M., & Tabuchi, H. (2004). The role of subsurface water flow paths on hillslope hydrological processes, landslides and landform development in steep mountains of Japan. *Hydrological Processes*, 18(4), 637–650.
- Oshun, J., Dietrich, W. E., Dawson, T. E., & Fung, I. (2016). Dynamic, structured heterogeneity of water isotopes inside hillslopes. *Water Resources Research*, 52, 164–189. <https://doi.org/10.1002/2015WR017485>
- Payn, R. A., Gooseff, M. N., McGlynn, B. L., Bencala, K. E., & Wondzell, S. M. (2012). Exploring changes in the spatial distribution of stream base flow generation during a seasonal recession. *Water Resources Research*, 48, W04519. <https://doi.org/10.1029/2011WR011552>
- Persendt, F. C., & Gomez, C. (2016). Assessment of drainage network extractions in a low-relief area of the Cuvelai Basin (Namibia) from multiple sources: LiDAR, topographic maps, and digital aerial orthophotos. *Geomorphology*, 260, 32–50.
- PRISM. (2010). PRISM Climate Group 30-Year Normals. Corvallis, OR: Oregon State University. Retrieved from <http://prism.oregonstate.edu>

- Price, K., Jackson, C. R., Parker, A. J., Reitan, T., Dowd, J., & Cyterski, M. (2011). Effects of watershed land use and geomorphology on stream low flows during severe drought conditions in the southern Blue Ridge Mountains, Georgia and North Carolina, United States. *Water Resources Research*, 47, W02516. <https://doi.org/10.1029/2010WR009340>
- Power, M. E., Parker, M. S., & Dietrich, W. E. (2008). Seasonal reassembly of a river food web: Floods, droughts, and impacts of fish. *Ecological Monographs*, 78(2), 263–282.
- Queener, N., & Stubblefield, A. P. (2016). Spatial and temporal variability in base flow in the Mattole River Headwaters, California, USA. *Hydrology and Earth System Sciences Discussions*, 1–39. <https://doi.org/10.5194/hess-2016-300>
- Rantz, S. E. (1968). *Average annual precipitation and runoff in north coastal California* (Hydrologic Atlas 298). Reston, VA: U.S. Geological Survey.
- Ray, R. A., Holt, R. A., & Bartholomew, J. L. (2012). Relationship between temperature and Ceratomyxa shasta-induced mortality in Klamath River salmonids. *Journal of Parasitology*, 98(3), 520–526.
- Reed, M. S., Buenemann, M., Athlapheng, J., Akhtar-Schuster, M., Bachmann, F., Bastin, G., et al. (2011). Cross-scale monitoring and assessment of land degradation and sustainable land management: A methodological framework for knowledge management. *Land Degradation & Development*, 22(2), 261–271.
- Rempe, D. M. (2016). *Controls on critical zone thickness and hydrologic dynamics at the hillslope scale* (doctoral dissertation). Berkeley, CA: University of California.
- Rempe, D. M., & Dietrich, W. E. (2014). A bottom-up control on fresh-bedrock topography under landscapes. *Proceedings of the National Academy of Sciences of the United States of America*, 111(18), 6576–6581.
- Rempe, D. M., & Dietrich, W. E. (2018). Direct observations of rock moisture, a hidden component of the hydrologic cycle. *Proceedings of the National Academy of Sciences of the United States of America*, in press. <https://doi.org/10.1073/pnas.1800141115>
- Rempe, D. M., Hahm, W. J., & Dietrich, W. E. (2015). *Oxidation of landscapes*. Abstract EP33D-04 presented at AGU Fall Meeting (Vol. 1, p. 4). Washington, DC: American Geophysical Union.
- Rempe, D. M., Oshun, J., Dietrich, W. E., Salve, R., & Fung, I. (2010). *Controls on the weathering front depth on hillslopes underlain by mudstones and sandstones*. Abstract EP34A-05 presented at AGU Fall Meeting (Vol. 1, p. 5). Washington, DC: American Geophysical Union.
- Riebe, C. S., Hahm, W. J., & Brantley, S. L. (2017). Controls on deep critical zone architecture: A historical review and four testable hypotheses. *Earth Surface Processes and Landforms*, 42(1), 128–156.
- Roering, J. J., Mackey, B. H., Handwerger, A. L., Booth, A. M., Schmidt, D. A., Bennett, G. L., et al. (2015). Beyond the angle of repose: A review and synthesis of landslide processes in response to rapid uplift, Eel River, Northern California. *Geomorphology*, 236, 109–131.
- Salve, R., Rempe, D. M., & Dietrich, W. E. (2012). Rain, rock moisture dynamics, and the rapid response of perched groundwater in weathered, fractured argillite underlying a steep hillslope. *Water Resources Research*, 48, W11528. <https://doi.org/10.1029/2012WR012583>
- Schaaf, C. J., Kelson, S. J., Nusslé, S. C., & Carlson, S. M. (2017). Black spot infection in juvenile steelhead trout increases with stream temperature in northern California. *Environmental Biology of Fishes*, 100(6), 733–744.
- Scheingross, J. S., Winchell, E. W., Lamb, M. P., & Dietrich, W. E. (2013). Influence of bed patchiness, slope, grain hiding, and form drag on gravel mobilization in very steep streams. *Journal of Geophysical Research: Earth Surface*, 118, 982–1001. <https://doi.org/10.1002/jgrf.20067>
- Seidl, M. A., & Dietrich, W. E. (1992). The problem of channel erosion into bedrock. *Catena Supplement*, 23, 101–124.
- Shaw, S. B. (2016). Investigating the linkage between streamflow recession rates and channel network contraction in a mesoscale catchment in New York State. *Hydrological Processes*, 30(3), 479–492.
- Shaw, S. B., Bonville, D. B., & Chandler, D. G. (2017). Combining observations of channel network contraction and spatial discharge variation to inform spatial controls on base flow in Birch Creek, Catskill Mountains, USA. *Journal of Hydrology: Regional Studies*, 12, 1–12.
- Sklar, L. S., & Dietrich, W. E. (2004). A mechanistic model for river incision into bedrock by saltating bed load. *Water Resources Research*, 40, W06301. <https://doi.org/10.1029/2003WR002496>
- Sklar, L. S., & Dietrich, W. E. (2008). Implications of the saltation–abrasion bedrock incision model for steady-state river longitudinal profile relief and concavity. *Earth Surface Processes and Landforms*, 33(7), 1129–1151.
- Sheets, R. A., Hill, M. C., Haitjema, H. M., Provost, A. M., & Masterson, J. P. (2015). Simulation of water-table aquifers using specified saturated thickness. *Groundwater*, 53(1), 151–157.
- St. Clair, J. S., Moon, S., Holbrook, W. S., Perron, J. T., Riebe, C. S., Martel, S. J., et al. (2015). Geophysical imaging reveals topographic stress control of bedrock weathering. *Science*, 350(6260), 534–538.
- Strauch, M., Lima, J. E., Volk, M., Lorz, C., & Makeschin, F. (2013). The impact of Best Management Practices on simulated streamflow and sediment load in a Central Brazilian catchment. *Journal of Environmental Management*, 127, S24–S36.
- Stock, J., & Dietrich, W. E. (2003). Valley incision by debris flows: Evidence of a topographic signature. *Water Resources Research*, 39(4), 1089. <https://doi.org/10.1029/2001WR001057>
- Stock, J. D., & Dietrich, W. E. (2006). Erosion of steepland valleys by debris flows. *Geological Society of America Bulletin*, 118(9–10), 1125–1148.
- Stock, J. D., Montgomery, D. R., Collins, B. D., Dietrich, W. E., & Sklar, L. (2005). Field measurements of incision rates following bedrock exposure: Implications for process controls on the long profiles of valleys cut by rivers and debris flows. *Geological Society of America Bulletin*, 117(1–2), 174–194.
- Sun, N., Yearsley, J., Voisin, N., & Lettenmaier, D. P. (2015). A spatially distributed model for the assessment of land use impacts on stream temperature in small urban watersheds. *Hydrological Processes*, 29(10), 2331–2345.
- Tague, C., & Grant, G. E. (2004). A geological framework for interpreting the low-flow regimes of Cascade streams, Willamette River Basin, Oregon. *Water Resources Research*, 40, W04303. <https://doi.org/10.1029/2003WR002629>
- Tilley, F. B., & Rice, R. M. (1977). *Casper Creek watershed study: A current status report* (State Forest Notes 66, 15 p.). Sacramento, CA: State of California, Department of Forestry.
- Tóth, J. (1963). A theoretical analysis of groundwater flow in small drainage basins. *Journal of Geophysical Research*, 68(16), 4795–4812.
- Troch, P. A., Paniconi, C., & Emiel van Loon, E. (2003). Hillslope-storage Boussinesq model for subsurface flow and variable source areas along complex hillslopes: 1. Formulation and characteristic response. *Water Resources Research*, 39(11), 1316. <https://doi.org/10.1029/2002WR001728>
- Ukar, E., & Cloos, M. (2016). Graphite-schist blocks in the Franciscan Mélange, San Simeon, California: Evidence of high-P metamorphism. *Journal of Metamorphic Geology*, 34(3), 191–208.
- Underwood, M. B. (1983). Depositional setting of the Paleogene Yager formation, northern Coast Ranges of California. In D. K. Larue & R. J. Steel (Eds.), *Cenozoic marine sedimentation, Pacific margin, U.S.A.: Pacific Section, SEPM* (pp. 81–101).

- Webb, B. W., Clack, P. D., & Walling, D. E. (2003). Water–air temperature relationships in a Devon river system and the role of flow. *Hydrological Processes*, 17(15), 3069–3084.
- Weitzell, R. E., Kaushal, S. S., Lynch, L. M., Guinn, S. M., & Elmore, A. J. (2016). Extent of Stream Burial and Relationships to Watershed Area, Topography, and Impervious Surface Area. *Water*, 8(11), 538.
- Welch, L. A., & Allen, D. M. (2012). Consistency of groundwater flow patterns in mountainous topography: Implications for valley bottom water replenishment and for defining groundwater flow boundaries. *Water Resources Research*, 48, W05526. <https://doi.org/10.1029/2011WR010901>
- Whiting, J. A., & Godsey, S. E. (2016). Discontinuous headwater stream networks with stable flow heads, Salmon River basin, Idaho. *Hydrological Processes*, 30, 2305–2316.
- Wigington, P. J., Moser, T. J., & Lindeman, D. R. (2005). Stream network expansion: A riparian water quality factor. *Hydrological Processes*, 19(8), 1715–1721.
- Willenbring, J. K., Gasparini, N. M., Crosby, B. T., & Brocard, G. (2013). What does a mean? The temporal evolution of detrital cosmogenic denudation rates in a transient landscape. *Geology*, 41(12), 1215–1218.
- Zimmer, M. A., & McGlynn, B. L. (2017). Ephemeral and intermittent runoff generation processes in a low relief, highly weathered catchment. *Water Resources Research*, 53, 7055–7077. <https://doi.org/10.1002/2016WR019742>